Article

Developmental Cell

Damage-responsive neuro-glial clusters coordinate the recruitment of dormant neural stem cells in *Drosophila*

Graphical abstract

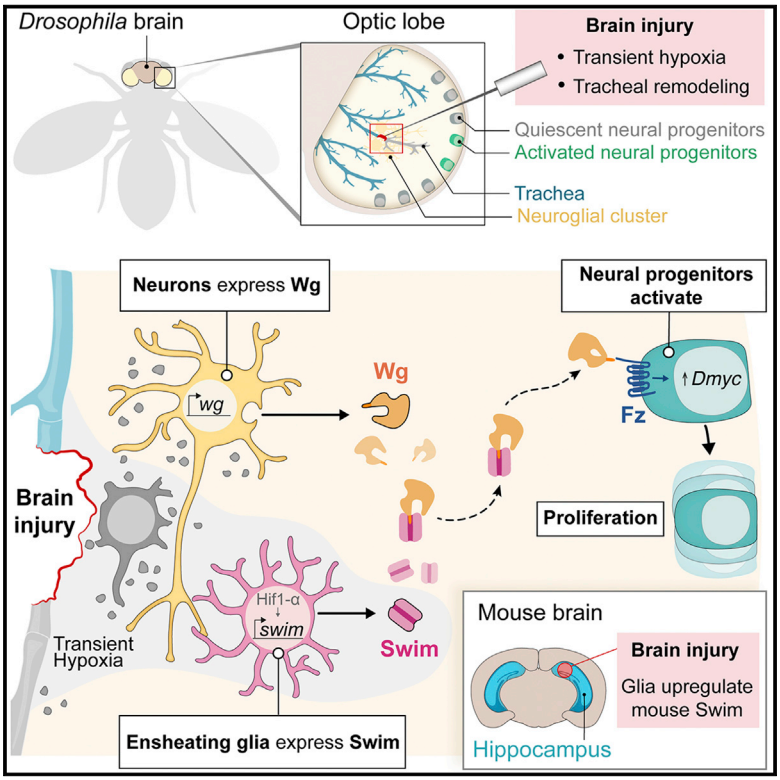

Highlights

- Brain lesions trigger a local coordinated response in neuro-glial clusters
- Glia produce the secreted transporter Swim upon transient brain hypoxia
- Swim promotes Wg/Wnt distribution in the injured brain domain
- Wg/Wnt signaling drives proliferation of normally quiescent neural stem cells

Authors

Anabel R. Simões, Marta Neto, Carolina S. Alves, ..., Irene Durá, Juan M. Encinas, Christa Rhiner

Correspondence

christa.rhiner@research.fchampalimaud.org

In brief

Simões et al. investigate adult brain plasticity in response to injury. They describe a mechanism by which neurons and glia cooperate to reactivate quiescent neural progenitors and promote a regenerative response. The process is based on a Hif1-α/Swim/Wnt signaling module that connects injury sensing to stem cell recruitment.

Simões et al., 2022, Developmental Cell *57*, 1–15
July 11, 2022
https://doi.org/10.1016/j.devcel.2022.05.015

CellPress

Please cite this article in press as: Simões et al., Damage-responsive neuro-glial clusters coordinate the recruitment of dormant neural stem cells in *Drosophila*, Developmental Cell (2022), https://doi.org/10.1016/j.devcel.2022.05.015

Developmental Cell

CellPress
OPEN ACCESS

Article

Damage-responsive neuro-glial clusters coordinate the recruitment of dormant neural stem cells in *Drosophila*

Anabel R. Simões,[1] Marta Neto,[1] Carolina S. Alves,[1] Mariana B. Santos,[1] Ismael Fernández-Hernández,[2] Henrique Veiga-Fernandes,[1] David Brea,[1] Irene Durá,[3,4] Juan M. Encinas,[3,4,5] and Christa Rhiner[1,6,*]

[1]Champalimaud Research, Champalimaud Foundation, 1400-038 Lisbon, Portugal
[2]Institute of Cell Biology, University of Bern, 3012 Bern, Switzerland
[3]Achucarro Basque Center for Neuroscience, 48940 Leioa, Spain
[4]Department of Neurosciences, University of the Basque Country (UPV/EHU), 48940 Leioa, Spain
[5]IKERBASQUE, The Basque Foundation for Science, 48009 Bilbao, Spain
[6]Lead contact
*Correspondence: christa.rhiner@research.fchampalimaud.org
https://doi.org/10.1016/j.devcel.2022.05.015

SUMMARY

Recruitment of stem cells is crucial for tissue repair. Although stem cell niches can provide important signals, little is known about mechanisms that coordinate the engagement of disseminated stem cells across an injured tissue. In *Drosophila*, adult brain lesions trigger local recruitment of scattered dormant neural stem cells suggesting a mechanism for creating a transient stem cell activation zone. Here, we find that injury triggers a coordinated response in neuro-glial clusters that promotes the spread of a neuron-derived stem cell factor via glial secretion of the lipocalin-like transporter Swim. Strikingly, *swim* is induced in a *Hif1-α*-dependent manner in response to brain hypoxia. Mammalian Swim (Lcn7) is also upregulated in glia of the mouse hippocampus upon brain injury. Our results identify a central role of neuro-glial clusters in promoting neural stem cell activation at a distance, suggesting a conserved function of the HIF1-α/Swim/Wnt module in connecting injury-sensing and regenerative outcomes.

INTRODUCTION

Injury is known to stimulate diverse forms of plasticity (Tetteh et al., 2015; Blanpain and Fuchs, 2014), which serve to restore organ function. Many tissues harbor a small number of undifferentiated adult stem cells that are engaged in tissue turnover or become activated following injury to replace damaged cells. Some tissues, such as muscle or brain, contain mainly dormant stem cells that are not dividing and reside in a reversible state of quiescence (van Velthoven and Rando, 2019). Niche cells in intimate contact with quiescent stem cells have been found to provide activating cues upon tissue damage (Fuchs and Blau, 2020; Wells and Watt, 2018; Chaturvedi et al., 2017). However, little is known how the activation of multiple dispersed stem cell units is coordinated to establish an adequate stem cell response zone across an injured tissue.

Quiescent progenitor cells in muscle and the brain respond to injury in mammals, but also in fruit flies (*Drosophila*) (Chaturvedi et al., 2017; Schwartz and Rhiner, 2018). This allows to harness the extensive genetic tools available in *Drosophila* to dissect injury-dependent stem cell activation. Although still unclear, the presence of dormant stem cells in short-lived insects indicates that these cells may play a beneficial role for tissue plasticity or repair upon predator attacks or inter-species aggressions (Chiu et al., 2021; Zwarts et al., 2012).

In the adult fly brain, experimental stab lesions to the optic lobes (OLs) or the central brain trigger a proliferative response resulting in local neurogenesis several days after injury (AI), which has been linked to activation of normally quiescent neural progenitor cells (qNPs) (Crocker et al., 2021; Fernández-Hernández et al., 2021; Moreno et al., 2015; Fernández-Hernández et al., 2013). qNPs have also been found to promote adult brain plasticity in contexts unrelated to injury (Li et al., 2020). On the other hand, stab lesions can also trigger glial divisions shortly after injury (Kato et al., 2009; Crocker et al., 2021).

Despite extensive knowledge on neural stem cell proliferation during fly development (Yaghmaeian Salmani and Thor, 2020; Nériec and Desplan, 2016; Homem et al., 2015; Sousa-Nunes et al., 2010), the signals governing qNP activation in response to injury are unknown. A ubiquitous pulse of *Drosophila Myc* (*dMyc*) overexpression has been previously shown to promote qNP division, but the signals detected by qNPs remained enigmatic (Fernández-Hernández et al., 2013).

In mammals, a wide variety of signals are known to regulate quiescent neural stem cells (qNSCs) in homeostatic conditions (Braun and Jessberger, 2014), whereas their response to tissue

Please cite this article in press as: Simões et al., Damage-responsive neuro-glial clusters coordinate the recruitment of dormant neural stem cells in *Drosophila*, Developmental Cell (2022), https://doi.org/10.1016/j.devcel.2022.05.015

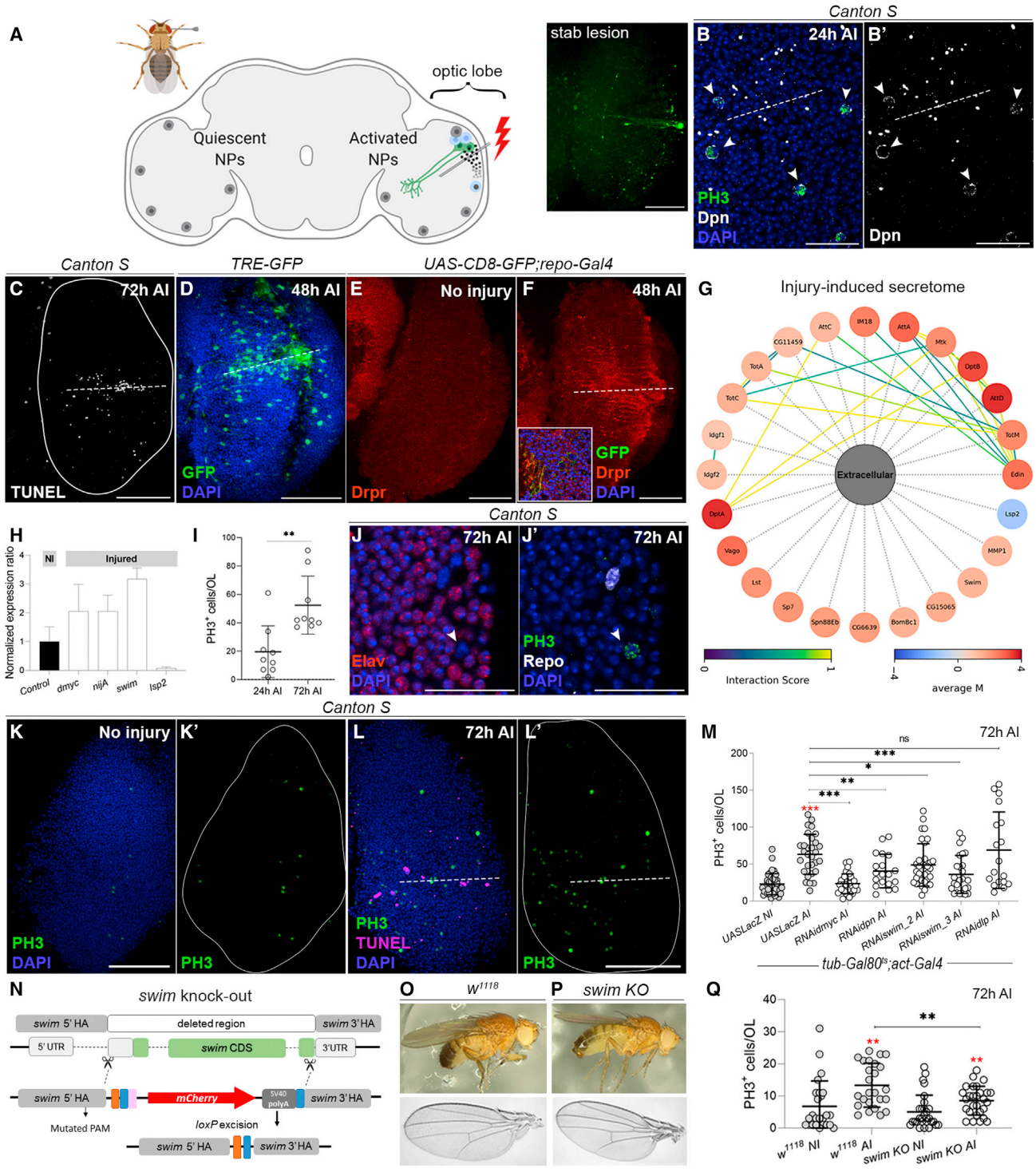

Figure 1. Secreted factors in the injured fly brain

(A) Scheme depicting stab lesion via the eye to the medulla of the optic lobe (OL). Quiescent neural progenitors (NPs) are depicted in gray, active NPs in blue. The needle trace is shown on the right with dye labeling.

(B) Dpn-expressing cells (arrowheads, white) with PH3 labeling (green). Injury sites are marked by a white dotted line in all panels.

(C) Apoptotic cells (white, TUNEL) 72 h after injury (AI).

(D) JNK pathway activation (*TRE::gfp*) 48 h AI.

(E and F) Draper expression (Drpr, red) in non-injured (E) and injured (F) OLs. Inset shows colocalization of Drpr with glial cells (*repo-gal4; UASCD8::gfp*) (green). DAPI highlights nuclei (blue).

(legend continued on next page)

Please cite this article in press as: Simões et al., Damage-responsive neuro-glial clusters coordinate the recruitment of dormant neural stem cells in *Drosophila*, Developmental Cell (2022), https://doi.org/10.1016/j.devcel.2022.05.015

damage is less well understood. qNSCs are located in two main niches, the subventricular zone and the dentate gyrus of the hippocampus, buried within the brain (Zhao et al., 2008). Upon brain injury, qNSCs only partially enter an activated state (Llorens-Bobadilla et al., 2015), and neuroblast recruitment to infarcted brain regions and local neurogenesis is limited (Arvidsson et al., 2002; Magnusson et al., 2014).

Strikingly, the initial consequences triggered by brain injury, which include neural cell death, upregulation of antioxidant defense, and c-Jun N-terminal kinase (JNK) stress signaling (Leyssen et al., 2005; Moreno et al., 2015; Saikumar et al., 2020; Ng and Lee, 2019), are very conserved in flies and mice suggesting that injury sensing of qNSCs/qNPs may rely on common principles.

Here, we studied injury-induced changes in the adult fly brain leading to recruitment of isolated qNPs near the injury site. We identify a crucial role of damage-responsive neuro-glial clusters (DNGCs), which enable proliferation of distant qNPs by promoting an enlarged stem cell activation zone. We provide evidence that these multicellular units orchestrate the spatial and temporal availability of an essential, but localized stem cell factor for qNPs via injury-stimulated secretion of the transport protein Swim. As Swim production is dependent on the injury-sensitive transcription factor HIF1-α, the identified mechanism may serve to spatially and temporary adjust the stem cell activation zone to the extent of damage suffered in a given tissue area, resulting in locally calibrated pulses of stem cell activity.

RESULTS

Acute brain injury induces prominent changes in secreted factors

To study how dormant neural progenitor cells are engaged by local brain injury, we focused on previously identified qNPs in the adult OL, which have been shown to express the HES type transcription factor Deadpan (Dpn) (Li et al., 2020; Fernández-Hernández et al., 2013). Dpn-expressing cells represent a very rare cell type in the adult brain (Konstantinides et al., 2018; Davie et al., 2018) and are scattered throughout the medulla cortex of the OLs without apparent niche (Fernández-Hernández et al., 2013; Figures 1A and 1B). Previous work has shown that stab lesions trigger a neurogenic response in the injured brain area. Interestingly, undifferentiated qNPs have been found in clusters of cells that proliferated specifically around the lesion site. Although normally quiescent, NPs in the injured OL area expressed the mitotic marker phosphohistone H3 (PH3) (Figure 1B), showed high dMyc levels and formed doublets (Fernández-Hernández et al., 2013), suggesting that they were recruited to repair.

Using dye labeling, we confirmed that previously established stab lesions target a relatively small area of the OL medulla (Figure 1A). The location of the lesion was alternatively monitored by the presence of weakly fluorescent pigment traces introduced by the needle from the eye (see STAR Methods). The puncture triggered apoptosis, typically 5–10 μm from the lesion site (Figure 1C) and activation of the JNK stress pathway in a more extensive area (10–20 μm away) (Figure 1D), in a volume amounting on average to 6% of the OL (n = 8 OLs) (see also Moreno et al., 2015; Fernández-Hernández et al., 2013). In addition, we found upregulation of the engulfment receptor Draper/Ced1, shown to promote clearance of neuronal debris in the adult brain (MacDonald et al., 2006) on glial cells (Figures 1E and 1F) but did not detect obvious alterations in glial morphology.

Due to their low density in the tissue, NPs were rarely found in direct contact with localized tissue damage suggesting that they were alerted to injury at some distance. We therefore speculated that injury resulted in the generation of a diffusible signal able to travel to nearby qNPs, but not distant progenitors outside the injured brain domain (Figure 1A).

To identify such cues, we conducted genome-wide transcriptional profiling of injured and intact adult fly brains. Overall, we detected 74 upregulated and 8 downregulated genes 48 h following OL injury, which we considered as high-confidence candidates ($1.3 > \log_2 FC < -1.3$; p value < 0.05) (Table S1; Figure S1A). Remarkably, most differentially expressed genes were associated with the extracellular space, revealing a specific injury-induced secretome (Figure 1G). From the functional side, the majority of injury-regulated genes grouped fell into the gene ontology terms immune and stress responses (Figure S1B). *Ninjurin A* (*NijA*) ranged among the significantly upregulated genes in lesioned brains (Table S1). NijA is a conserved transmembrane protein strongly induced by nerve injury in axons and Schwann cells in mice (Araki and Milbrandt, 1996). Using a NijA-specific antibody, we found marked NijA upregulation in injured fly brains, which was absent in injured *nijA*null mutants (Broderick et al., 2012; Figures S1C–S1E).

Given our interest in diffusible factors, we next focused on the injury-induced secretome, which comprised innate immunity and stress-associated factors (*diptericins, attacins, cecA1, vago, mtk, turandots, edin, sp7, bbd*, and *bomS5*), modulators of insulin signaling (*Ist* and *idgfs*), cell adhesion (*mmp1*), and extracellular transport (*swim*) (Figure 1G). Among the most

(G) Injury-induced secretome. Induction based on M values (highest red, lowest blue). Interactions are indicated with lines (yellow high, blue low).
(H) qRT-PCR for selected targets, n = 3, error bars show SEM.
(I) PH3+ cells 24 and 72 h AI. n = 9 OLs.
(J) NP marked by anti-PH3 staining (green), Elav is shown in red (J), and Repo in white (J′).
(K and L) PH3 signal in non-injured (K) and injured (L) OLs. Apoptotic cells are marked with TUNEL (magenta) (L).
(M) Conditional activation of RNAi with *tub-Gal80^{ts}; act-Gal4* in adult flies prior to injury. Quantification of injury-induced proliferation (PH3+ cells) 72 h AI. NI, non-injured; AI, injured. n $\geq$ 20 OLs.
(N) CRISPR-Cas9-mediated knockout strategy used to generate *swim$^{3.3}$* KO flies. Small ellipses (blue) indicate *loxP* sites flanking the *mCherry* transgenesis marker.
(O and P) (O) Adult control (*w^{1118}*) and *swim$^{3.3}$* KO fly (P) and respective wings.
(Q) PH3 counts in intact and injured (72 h AI) OLs of control and *swim$^{3.3}$ KO* flies. n $\geq$ 25 optic lobes. Red asterisks depict significant differences between the non-injured (NI) and injured (AI) state. Error bars for PH3 counts depict SD. *p < 0.05; **p < 0.01, ***p < 0.001. ns, not significant. Scale bars, 50 μm in (A), (C), (D), and (K) and 20 μm in (B) and (J).

Please cite this article in press as: Simões et al., Damage-responsive neuro-glial clusters coordinate the recruitment of dormant neural stem cells in *Drosophila*, Developmental Cell (2022), https://doi.org/10.1016/j.devcel.2022.05.015

downregulated genes was *lsp2*, previously identified as repellent cue for axonal outgrowth at the neuromuscular junction (Inaki et al., 2007).

Based on its role as extracellular transport protein, Swim represented an interesting factor potentially able to spread local injury cues. We therefore performed independent quantitative expression analysis, which confirmed injury-dependent *swim* upregulation (Figure 1H). Lesioned brains also showed increased levels of *NijA* and *myc*, previously associated with qNP activation (Fernández-Hernández et al., 2013) and reduced *lsp2* expression, suggesting that our previous transcriptional profiling of injured brains provided a faithful overview on major regulated targets.

Swim regulates proliferation in the injured brain

Swim is a lipocalin-like protein, which can facilitate extracellular transport of hydrophobic molecules. It was previously found to strongly bind to and increase solubility of secreted lipid-modified Wg/Wnt *in vitro* (Mulligan et al., 2012).

As Wg/Wnt are important stem cell factors, we set out to test if Swim was important to promote the regenerative response.

We monitored injury-induced proliferation of qNPs, with PH3 staining 72 h AI, at the peak of the proliferative response (Figure 1I). PH3+ progenitors were undifferentiated and did not express neuronal or glial markers (ELAV and Repo, respectively) (Figure 1J). The majority of PH3+ cells were detected near the area of cell death induced by the puncture (Figures 1K and 1L). Similarly, EdU incorporation, which marks cells in S phase, was mainly observed in cells in the vicinity of the lesion site (Figures S1F and S1G). We detected very few PH3+ glia 72 h AI (0.1 cell/OL, n = 8 OLs) compared with 24 h AI (1.5 ± 0.8 cells/OL, n = 8 OLs) (Figure S1H) suggesting that glia mainly divided in the acute phase AI.

To test a role of *swim* in injury-induced proliferation, we conditionally activated RNAi against *swim* in adult *tub-Gal80^{ts}; act-Gal4/UASswimRNAi* flies prior to injury relying on the temperature-sensitive (ts) Gal4 suppressor Gal80^{ts} and performed PH3+ counts 72 h AI. We counted all cells with PH3 signal independent of signal intensity and considered non-injured (NI) brains as a baseline for injury-induced proliferation (Figure 1M). Interestingly, *swim* knockdown with two different RNAi lines resulted in significant suppression of injury-induced proliferation as did RNAi of *dpn*, whereas *RNAi* of *myc* resulted in an even stronger reduction of PH3 signal. In contrast, knockdown of *dally-like* (*dlp*), a Wg-interacting protein in developing epithelia (McGough et al., 2020), did not alter PH3 counts.

To address whether Swim may be generally required for proliferation, we analyzed flies in which *swim* levels were knocked down from early development, which did not interfere with development or adult brain morphology (Figures S1I and S1J). A small fraction of *swim* RNAi flies displayed partially blistered wings, but this was only observed with one of the two *swim* RNAi lines used. In turn, ubiquitous *swim* overexpression caused slightly larger wings, likely related to the mitogenic effect of Wg/Wnt signaling during wing disc development (Neumann and Cohen, 1996; Baena-Lopez et al., 2009) (Figures S1K and S1L). To study complete *swim* loss of function, we next generated *swim*null flies by removing the entire *swim* coding region via CRISPR-Cas9-directed gene editing (Huang et al., 2009; Figure 1N; Figure S1M). Remarkably, brains of adult *swim$^{3.3}$* knockout (KO) flies did not show defects in morphology or cellular composition, and wings were comparable to controls (Figures 1O and 1P; Figures S1N and S1O). However, when they were challenged with stab lesions, *swim* KO flies showed a marked deficit in injury-induced proliferation (Figure 1Q; Figure S1P) in line with previous *swim* RNAi results (Figure 1M). This was not caused by a generally reduced tissue fitness as *swim* KOs did not show different mortality after wounding compared with injured controls (Figure S1Q). However, *swim KO* showed defects in brain morphology (vacuoles) following injury pointing to a potentially reduced regenerative capacity compared with lesioned control flies (Figures S1R–S1T).

Overall, the results showed that Swim transporters were largely dispensable for development and adult brain maintenance but critically required to mount a regenerative response to brain injury.

Injury activates a coordinated neuro-glial response

To pinpoint the cellular source of Swim, we created a *swim* reporter line by knocking in tagged *swim* coding sequences into *swim* KO flies under the control of endogenous *swim* enhancer sequences (*swim* KI *{swim KO; swim::mCherry}*) (Figure 2A). At embryonic stage, Swim::mCherry was expressed in multiple tissues, in line with *in situ* resources (Figures S2A–S2D). In larvae, Swim::mCherry was highly expressed in secretory pericardial nephrocytes. Low levels were also detected in developing wing epithelia (Figures S2E and S2F). In the adult OLs, *swim::mCherry* was barely expressed under homeostatic conditions, in agreement with available single-cell data (Konstantinides et al., 2018). However, following brain injury, we observed a potent increase of the mCherry signal and return to baseline by 1 week AI (Figures 2B–2D). Staining with cell-type-specific markers revealed consistent induction of Swim::mCherry in Repo+ glial cells in the injured domain of the OL and never in Elav+ neurons (Figure 2E). We also sorted GFP-marked glia (*repo-Gal4; UASgfp*) and neurons (*elav-Gal4; UASgfp*) from injured and NI OLs and performed bulk RNA-seq, which detected *swim* expression exclusively in injured glia (Figure S2G). To experimentally test if Swim function was indeed required in glia to drive proliferation, we knocked down *swim* expression in adult glia using *tub-Gal80^{ts}; Repo-Gal4*. Remarkably, this resulted in drastically reduced cell divisions (Figure 2F) suggesting that glial-derived Swim transporters were essential to promote cell divisions following tissue damage. Interestingly, Swim was not induced in astroglia labeled by *alrm-gal4; UASgfp* (Figure S2H), but in injury-exposed ensheathing glia (*mz0709-gal4; UASgfp*), which can show extensive projections (Figures S2I and S2J).

Since Swim has been described to interact with Wg/Wnt, we examined whether *wg* activation was influenced by brain injury, using a *wg-Gal4* enhancer trap line shown to reflect endogenous *wg* expression (Calleja et al., 1996) in combination with nuclear-targeted GFP (*UASgfp*). We detected a significant increase of *wg*-driven GFP in injured OLs compared with intact adult OLs (Figures 2G–2I), which returned to baseline by 1 week AI (Figure 2I). Since Wg/Wnts released from dying cells have been shown to induce proliferation following tissue damage (Pérez-Garijo et al., 2009; Ryoo et al., 2004), we checked whether *wg*-expressing cells (GFP+) colocalized with apoptotic markers

Please cite this article in press as: Simões et al., Damage-responsive neuro-glial clusters coordinate the recruitment of dormant neural stem cells in *Drosophila*, Developmental Cell (2022), https://doi.org/10.1016/j.devcel.2022.05.015

CellPress
OPEN ACCESS

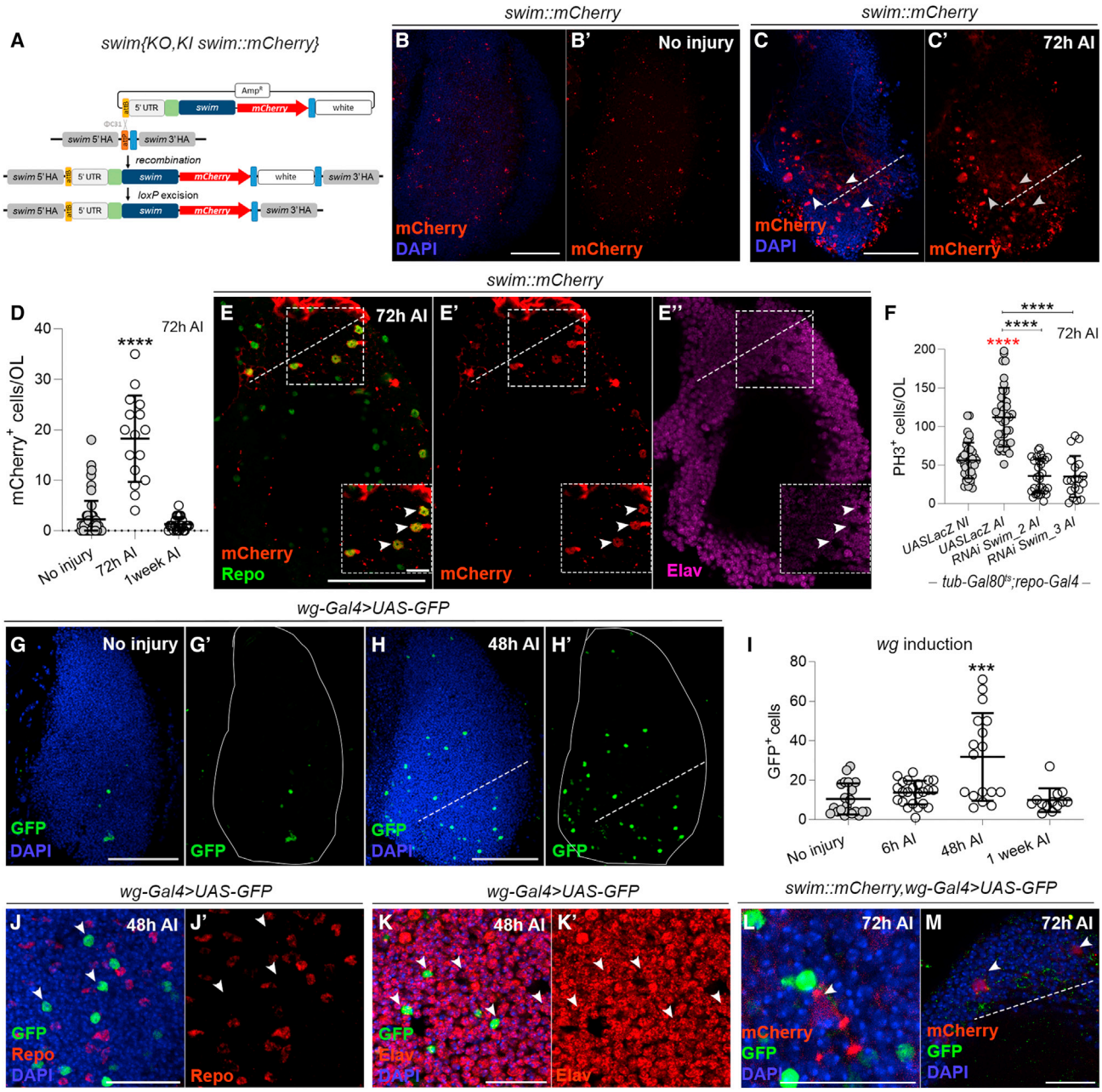

Figure 2. Injury induces the formation of Swim and Wg-expressing neuro-glial clusters

(A) CRISPR-Cas9-guided knockin of *mCherry*-tagged *swim* coding sequences into *swim* KO flies. Blue boxes mark *loxP* sites.

(B and C) Swim::mCherry expression in non-injured (B) and injured (C) adult optic lobes (OLs). White arrowheads mark Swim::mCherry-expressing cells. Dashed white line marks injury site.

(D) Number of Swim::mCherry+ cells in non-injured and injured OLs, 3 and 7 days after injury (AI). n ≥ 17 OLs. ****p < 0.0001.

(E) Swim::mCherry expression (red) is upregulated in glia upon injury. Insets show colocalization (arrowheads) of Swim (red) with glial Repo (green), but not with neuronal Elav+ (magenta).

(F) Injury-induced proliferation in the presence of *swim* RNAi in adult glia (*tub-Gal80^{ts}; repo-Gal4*). n ≥ 21. ****p < 0.0001.

(G and H) *Wg* expression (GFP) in intact (G) or lesioned (H) OLs. DAPI (blue) marks cell nuclei.

(I) Quantification of GFP+ cells (*wg-Gal4* and *UASgfp*) in non-injured and injured OLs. n ≥ 13 OLs. *** p < 0.001.

(J and K) *Wg* induction (GFP, arrowheads) is absent in glial cells (Repo+, red) (J), but occurs in neurons (Elav+, red) (K).

(L) Neuro-glial clusters (arrowheads) expressing *wg* (*wg-Gal4,UASgfp*) and Swim (mCherry) in the OL in response to injury. Inset: an axon in close contact with a Swim-expressing glia is shown.

(M) Injury-induced neuro-glial clusters in the OL (*swim::mcherry, wg::gfp*). All error bars are SD. Scale bars: 50 μM (B), (C), (E), (G), and (H) and 20 μM (J)–(M).

Please cite this article in press as: Simões et al., Damage-responsive neuro-glial clusters coordinate the recruitment of dormant neural stem cells in *Drosophila*, Developmental Cell (2022), https://doi.org/10.1016/j.devcel.2022.05.015

(TUNEL, Dcp-1), but this was not the case (Figures S2K and S2L). Further analyses with cell-type-specific markers showed that *wg*-driven GFP was not expressed in glia, but in a small subset of Elav+ neurons (Figures 2J and 2K).

Wg is normally not expressed in neurons in the adult fly brain (Konstantinides et al., 2018; Davie et al., 2018). To determine which neurons may show injury-dependent induction of *wg*, we assessed colocalization with neuronal-subset specific transcription factors. We found no evidence of *wg* upregulation (GFP) in Seven-up-expressing multicolumnar neurons but detected colocalization of *wg*-driven GFP with Brain-specific homeobox (Bsh) (Figures S2M and S2N), which is specifically expressed in unicolumnar Mi1 neurons in the adult OL (Erclik et al., 2017).

Strikingly, when *swim::mCherry* and *wg>gfp* expression were observed together at tissue scale, *wg*-expressing neurons and mCherry-expressing glia were located in close proximity, forming multicellular neuro-glial clusters of different size and compositions (Figures 2L and 2M).

We thus concluded that the proliferative response is governed by such hetero-cellular units that provide secreted factors (Swim and Wg) in a highly concerted manner.

Swim promotes Wg/Wnt distribution in the local tissue environment

To further explore the potential interaction of Swim with Wg/Wnt, we monitored Wg distribution with a Wg-specific antibody, which labels Wg-producing and Wg-binding cells. In the absence of damage, Wg signal was observed on few cells in adult OLs (Figure 3A). However, post injury, Wg could be detected on an increasing number of cells in the injured OL area (Figure 3B). We also injured *wg::gfp* flies (Port et al., 2014) to monitor expression of GFP-tagged Wg and found an injury-specific induction of Wg and increased localization of Wg in the lesioned OL area including on nearby qNPs (Figures S3A–S3C).

As lipid-modified Wg/Wnt cannot easily diffuse away from cell membranes (Nusse and Clevers, 2017), we tested whether Wg spread was dependent on Swim transporters (Figure 3C). Indeed, conditional activation of *actin*-driven *swim* RNAi in adult flies suppressed Wg distribution in injured OLs (Figures 3D–3F). In line with this, Wg signal was also markedly diminished in *swim* KO flies (Figures 3G–3I).

To assess if *swim* was not potentially required to stimulate Wg production in additional cells and therefore caused restricted Wg signal in *swim* mutants, we measured *wg* transcripts in injured *swim* KO flies but did not find impaired induction compared with controls (Figure S3C). Hence, we concluded that *swim* did not transcriptionally regulate *wg* expression but rather promoted transport of Wg from few *wg*-producing neurons (Figures 2H and 2K) to the local tissue environment. We therefore interrogated next whether extracellular travel of Wg ligands was involved to attain a broader range of Wg distribution following injury. To this end, we analyzed Wg distribution in injured *wg* KO flies expressing exclusively a membrane-tethered Wg form (*wg KO; NRT-Wg*) (Alexandre et al., 2014; Figure 3C). In these conditions of more limited Wg diffusion, Wg signal appeared again more localized (Figures 3J–3L). Correspondingly, PH3 counts were significantly lower (Figure 3M), indicating that both secreted Swim and diffusible Wg/Wnt were necessary to drive robust proliferation.

Taken together, we found that glial supply of Swim transporters promoted mobilization of Wg/Wnt and possibly also other lipid-modified growth factors to disseminated qNPs in the injured brain area.

qNPs are regulated by elevated Wg/Wnt signaling

Transport of Wg/Wnt promoted by neuro-glial clusters may allow Wg to reach dispersed qNPs, which normally are not exposed to it. To explore this idea, we first assessed whether manipulation of Wg signaling (Figure 4A) in adult flies with *tub-Gal80^{ts}*; *actin-Gal4* altered injury-induced proliferation. Knockdown of the activating ligand (*UASRNAi wg*, 2 copies) at adult stage strongly reduced cell divisions, as did *RNAi of myc* (Figure 4B). Remarkably, overexpression of a dominant-negative version of the Wg receptor Frizzled (*UASFz^{DN}*) and overexpression of *Drosophila* Axin (*UASdaxin*), a negative Wg pathway regulator, significantly suppressed PH3 counts following stab lesion. Accordingly, also overexpression of a dominant-negative version of TCF (*UASTCF^{DN}*), the effector transcription factor of the Wg/Wnt pathway prevented an efficient mitotic response to injury (Figure 4B) indicating that Wg signaling was required for proliferation. When we induced *actin*-driven *wg* expression prior to stab lesion, injury-induced proliferation increased even further (Figure 4B).

To further explore the link between injury and *wg* induction, we additionally examined the regenerative response in *wg^{1}* mutants (Morata and Lawrence, 1977) lacking a 2,416-bp spanning damage-responsive enhancer region (Harris et al., 2016). Strikingly, *wg^{1}* flies showed also impaired proliferation in response to injury compared with the control background (Figure 4C) indicating that *wg* induction in the lesioned brain depends on damage-responsive enhancer elements.

High levels of Wg/Wnt signaling within quiescent neural stem cells promotes their activation

The features of qNPs in the adult fly brain are still mostly unknown, including their regulation by external signals. In order to specifically target signals in these cells, we generated a *dpn*-dependent driver line relying on an approach shown to achieve robust expression in the adult brain (Diao and White, 2012): We inserted *gal4* sequences into the C terminus of the *dpn* locus with a co-translationally separating T2A peptide, allowing Gal4 to be co-expressed with endogenous Dpn (Figure 4D). *dpn::T2A::gal4* showed activity in known sites of Dpn expression such as in larval neuroblasts and growing imaginal wing discs (Figures S4A and S4B). As observed with conventional Dpn-Gal4 lines, inheritance of Gal4 and GFP molecules also labeled the progeny of dividing neuroblasts during development (Suzuki et al., 2016; Figure S4B). In the adult OLs, *dpnT2A-Gal4* labeled NPs as detected by Dpn staining or absence of Elav and Repo (Figures 4E and 4F) and Repo+ cells (Figure 4F), which might still express GFP following neuroblast-driven gliogenesis at the very end of OL development (Apitz and Salecker, 2014).

To suppress any potential developmental *dpn-T2A-Gal4* contribution, we added *tub-Gal80^{ts}*, which effectively blocked developmental *dpnT2A-Gal4* activity (Figure S4C) and combined

Please cite this article in press as: Simões et al., Damage-responsive neuro-glial clusters coordinate the recruitment of dormant neural stem cells in *Drosophila*, Developmental Cell (2022), https://doi.org/10.1016/j.devcel.2022.05.015

CellPress
OPEN ACCESS

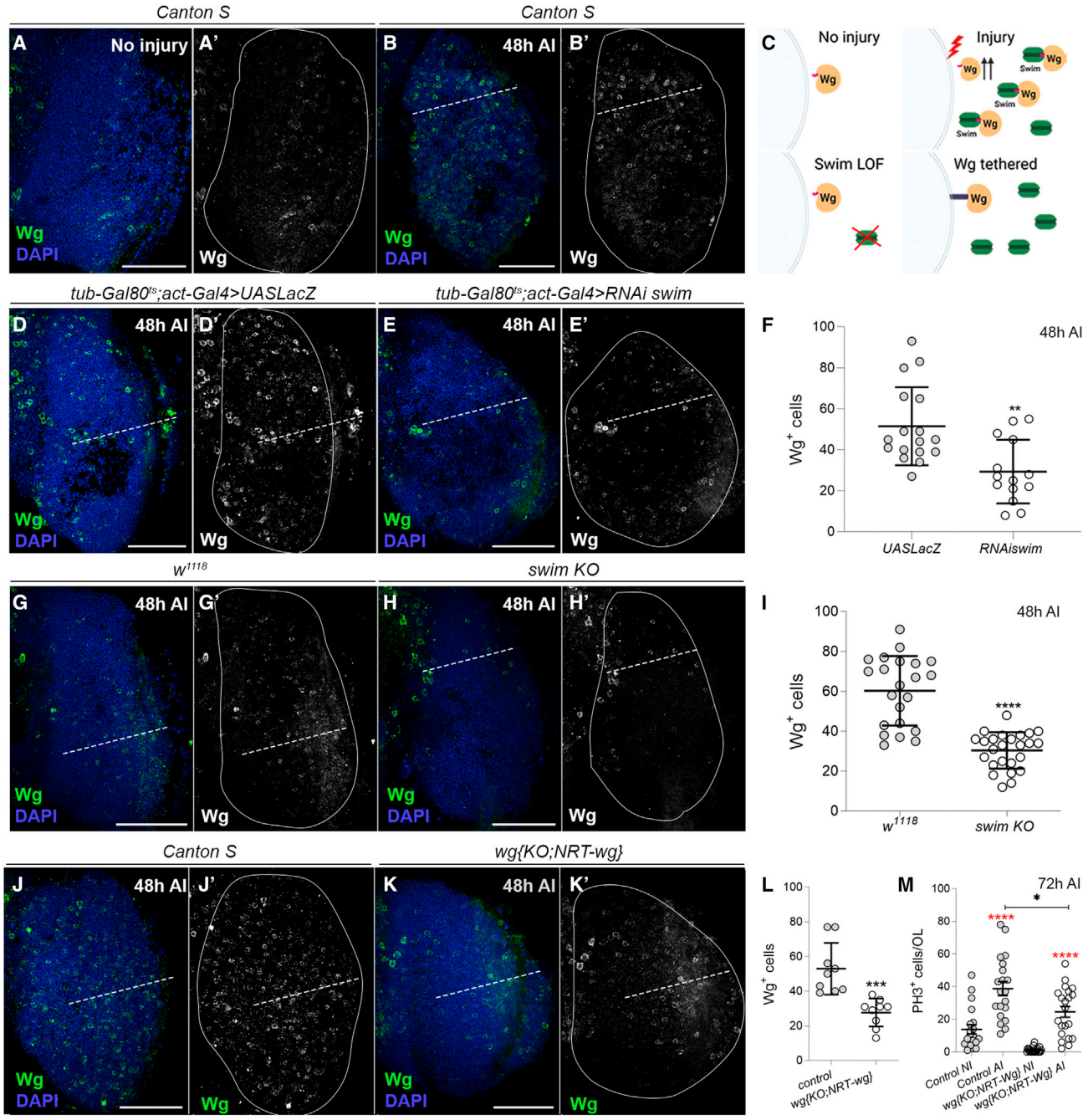

Figure 3. Swim promotes Wg mobilization in the injured brain area

(A and B) Wg signal (anti-Wg) in green (A and B) or white (A′ and B′) in non-injured optic lobes (OLs) (A) or 48 h after injury (AI) (B).

(C) Scheme illustrating tested Wg and Swim scenarios.

(D and E) Wg signal (green/white) following injury (48 h AI) in OLs with adult-onset induction of *UASlacZ* (D) or *UASswimRNAi* (E). Cell nuclei are shown in blue (DAPI). Dashed white line marks injury site.

(F) Wg+ cells per injured OL in control (*UASlacZ*) and *swim* RNAi flies crossed to *tub-Gal80^{ts}; act-Gal4*. n ≥ 14 OLs.

(G and H) Wg signal (green/white) in injured *swim$^{3.3}$* KO OLs (H) versus controls (*w^{1118}*) (G).

(I) Wg+ cells in injured OLs of control and *swim$^{3.3}$ KO* flies. n ≥ 25 OLs.

(J and K) Distribution of Wg signal (green/white) in injured controls (*Canton S*) (J) and injured *wg {KO; NRT-Wg}*) flies (K). Nuclei are shown in blue (DAPI).

(L) Wg+ cells in injured OLs of wild-type (*Canton S*) and *wg {KO; NRT-Wg}* flies. n ≥ 10 OLs.

(M) Injury-induced proliferation (PH3) in control (*Canton S*) and *wg {KO; NRT-Wg}* flies. n ≥ 20 OLs. AI: injured, NI: non-injured. All error bars show SD. *p < 0.05; **p < 0.01, ***p < 0.001, ****p < 0.0001. White lines highlight contours of adult OLs. Scale bars, 50 μM.

Please cite this article in press as: Simões et al., Damage-responsive neuro-glial clusters coordinate the recruitment of dormant neural stem cells in *Drosophila*, Developmental Cell (2022), https://doi.org/10.1016/j.devcel.2022.05.015

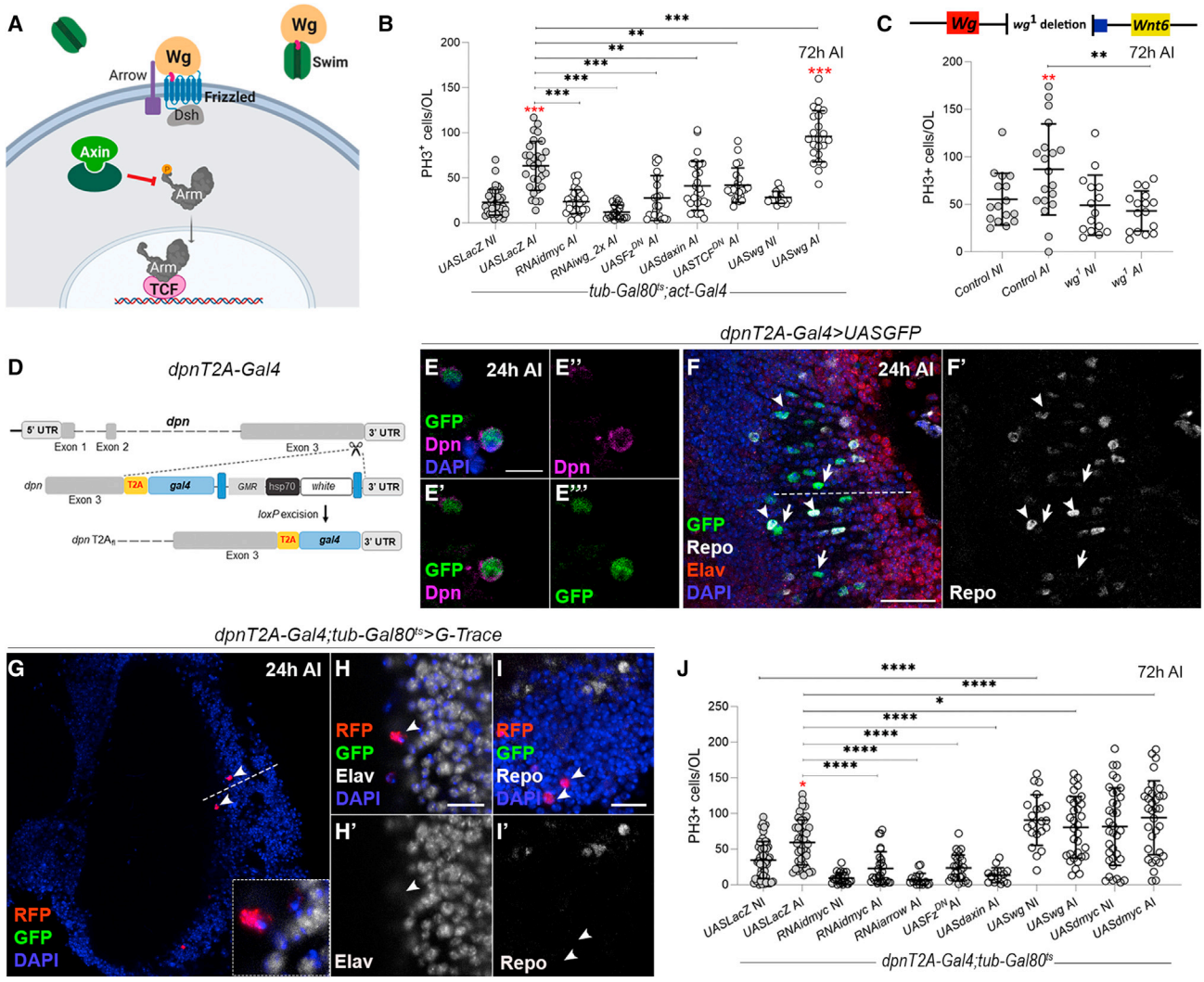

Figure 4. High levels of Wg and dMyc drive activation of qNPs

(A) Canonical Wg signaling in *Drosophila*.

(B) Wg/Wnt pathway manipulation in adult flies with *tub-Gal80^{ts}; act-Gal4*. PH3 counts in injured (72 h AI) or NI OLs. n ≥ 20 OLs.

(C) Top: deleted damage-responsive enhancer region in *wg^{1}* mutants. PH3+ cells in *Canton S* (control) and *wg^{1}* mutants 72 h AI. n ≥ 16 OLs.

(D) Schematic of C-terminally added *T2A-gal4* sequences to *dpn*. *gal4* is co-expressed with endogenous *dpn* by use of the viral ribosomal skipping site T2A leading to translation arrest and reinitiation after T2A. Blue boxes mark *loxP* sites flanking the *white*+ transgenesis marker.

(E) Dpn expression (anti-Dpn, magenta) in *dpn*::*T2A-Gal4*-labeled cells (GFP) in the adult OL.

(F) *dpn*::*T2A-Gal4*>GFP signal in adult OLs 24 h AI. White dashed line marks injury. Arrowheads identify GFP+/Repo+ cells and arrows GFP+/Repo− cells. Repo is shown in white, Elav signal in red, nuclei in blue (DAPI).

(G) Adult-onset *dpn* activation in *dpn*::*T2A*-Gal4; *tub-Gal80^{ts}* flies crossed to *UAS-G-trace*. Real-time *dpn* expression is shown in red (arrowheads) 24 h AI.

(H and I) *Dpn*-expressing cells (RFP+) neither express Repo (white) (I) nor Elav (white) (H).

(J) Manipulation of Wg signaling or dMyc expression in the adult brain and respective PH3 counts in non-injured (NI) and injured (72 h AI) OLs. n ≥ 25 OLs. Error bars show standard deviation. *p < 0.05; **p < 0.01, ***p < 0.001, ****p < 0.0001. Scale bars, 20 μM in (F), 10 μM (H) and (I), and 5 μM (E).

G-trace cassettes (Evans et al., 2009) to visualize real-time expression of *dpn* in RFP and *dpn*-derived progeny in GFP. Using this approach, we detected *dpn* expression (RFP) in undifferentiated progenitor cells (Repo-/Elav-) acutely AI (Figure 4G–4I). Dissected G-trace flies 1 week AI, contained GFP+ neurons (Elav+) in the OL medulla indicating an origin from previously *dpn*-expressing cells (Figure S4E).

When we analyzed features of cells marked by adult activation of *dpnT2A-Gal4* 24 h AI, we found that 90% of marked cells were undifferentiated NPs (Elav-Repo- or Dpn+) (Figures 4G–4I; Figure S4D) and 10% were Repo+ (n = 12 OLs).

These results showed that *dpnT2A-Gal4* efficiently targeted NPs but was also expressed in few glia or in a NP-related cell with glial features.

We then asked whether Wg/Wnt signaling was required in NPs by manipulating Wg pathway activity with adult-restricted *dpnT2A-Gal4*. Strikingly, RNAi of *myc* abolished the ability of qNPs to mount a proliferative response (Figure 4J). Similarly,

Please cite this article in press as: Simões et al., Damage-responsive neuro-glial clusters coordinate the recruitment of dormant neural stem cells in *Drosophila*, Developmental Cell (2022), https://doi.org/10.1016/j.devcel.2022.05.015

inhibition of the Wg receptors Frizzled (*UASFz* dominant negative) or Arrow (*arrow* RNAi) or overexpression of *Daxin* suppressed their proliferation following brain damage. On the other hand, cell-autonomous overexpression of Wg in *dpn*-expressing progenitors efficiently stimulated cell divisions even in the absence of injury. Likewise, overexpression of *myc* was sufficient to drive qNP activation without tissue damage (Figure 4J).

These results established that *dpn*-expressing cells in the adult fly brain can be effectively mobilized by Wg/Wnt signaling and elevated dMyc levels.

Swim is induced in a Hif1-alpha-dependent manner

What are the factors that control *swim* upregulation upon injury? In mammals, brain or nerve injuries result in rapid tissue hypoxia, which is thought to be caused by reduced perfusion and increased oxygen consumption of injured neurons (hyperactivation, ion leakage) (Lim et al., 2015; Hinzman et al., 2016).

As transcript levels of *lcn7/tinagl1*, the mammalian ortholog of *swim*, were altered by differential oxygen concentration (Perez-Perri et al., 2016), we tested whether *swim* induction is dependent on the hypoxia-responsive transcription factor HIF-1, formed by an O_2-sensitive α (HIF1-α) and a constitutive β subunit (Semenza, 1998; Lavista-Llanos et al., 2002). HIF1-α gains stability under hypoxia, whereas it is targeted for proteasomal degradation when oxygen is abundant (Jaakkola et al., 2001).

To probe if *swim* upregulation was dependent on *Hif1-α*, we assessed *swim* induction in null mutants of *Hif1-α*, called *sima* in *Drosophila*. In wild-type flies, *swim* transcripts rose 3-fold AI, whereas *swim* upregulation was not detectable in *sima* null flies (Centanin et al., 2005; Figure 5A). To further interrogate a possible link between brain injury and hypoxia-induced *swim* induction, we monitored tissue oxygenation in flies expressing the dynamic oxygen sensor protein nlsTimer (Lidsky et al., 2018; Figures 5B–5D). Maturation of nlsTimer into a red fluorescent form is strongly oxygen dependent (Figure 5B; Lidsky et al., 2018). Ratiometric image analyses (red versus green forms) showed ample presence of the red oxygen-dependent form in the NI OL, whereas the lesioned side displayed local hypoxia acutely after damage (24 h AI) (Figures 5C and 5D). No significant differences were detected at later time points. In addition, we also monitored GFP fused to the oxygen-dependent degradation domain (ODD) of HIF1-α, which allows monitoring of stabilized GFP under hypoxia (Misra et al., 2017). In accordance with previous results, GFP-ODD signal was specifically increased in OLs 24 h AI compared with the NI condition or later time points (Figures S5A–S5C). Strikingly, OL stab lesions also triggered consistent activation of *ldh-lacZ*, an HRE-based hypoxia sensor that is specifically induced under tissue hypoxia (Lavista-Llanos et al., 2002; Figure 5E).

To formally establish whether hypoxia was sufficient to trigger *swim* expression without injury, we transferred *swim::mCherry* larvae and adults for 6 or 24 h, respectively, to hypoxic chambers (5% O_2) (Figure 5F). Interestingly, we found that both in larvae and adult flies, hypoxia was sufficient to induce considerable *swim::mCherry* expression (Figures 5G and 5H). In contrast, *wg-Gal4, UASgfp* expression was not changed upon hypoxia (Figures S5D and S5E).

Hypoxia may be partly caused by impaired oxygen-perfusion of injured tracheal branches as a consequence of the stab lesion. Although we could not detect obvious damage in tracheal branches of lesioned OLs, we detected upregulation of Matrix metalloproteinase 1, a marker of tracheal remodeling (Glasheen et al., 2010), on airways in the injured brain side (Figure S5F).

In summary, these findings indicated that transcriptional induction of *swim* is regulated in a *hif1-α*-dependent manner, likely downstream of hypoxia created by brain lesions. Hif1-α could either directly activate *swim* transcription or indirectly via the regulation of other hypoxia-responsive factors.

Mouse Swim (Lcn7) is induced in glial cells of the hippocampus in response to brain injury

We then turned to mouse models of traumatic and ischemic brain injury to address whether the hypoxia-dependent injury-sensing mechanism that controls Swim expression is conserved in mammals. The function of the mammalian homolog of Swim, called Lipocalin 7 (Lcn7) is not known.

Strikingly, we found that traumatic brain injury (TBI) caused by controlled cortical impact led to induction of Lcn7 similarly to our observation of mechanical injury (TBI) in flies. Under homeostatic conditions, Lcn7 protein was not detectable in the hippocampus of control (anesthesia) or sham-operated mice (anesthesia and cortex exposure). In contrast, Lcn7 was clearly upregulated in the hippocampus of mice 3 days after TBI. Lcn7 signal overlapped with GFAP+ astrocytes of the dentate gyrus, but not with *nestin*-GFP labeled neuronal cells (Figures 5I–5L). We also found high levels of Lcn7 in the hippocampus of mice following stroke induction in one hemisphere using transient middle cerebral artery occlusion (MCAO) compared with the spared contralateral side (Jackman et al., 2011). Similarly, the Lcn7 signal was associated with ramifications of GFAP+ glial cells in the hippocampus (Figures 5M and 5N) showing that injury-induced Swim expression in glial cells was conserved in the mammalian brain. Our findings are in line with transcriptional data from mouse brains, which show significant *lcn7* induction upon stroke (Helton et al., 2005).

Together, these results suggest that the secretion of Swim/Lcn7 transporters in the hypoxic brain following injury is conserved in mammals.

DISCUSSION

How tissue damage is sensed and how the recruitment of multiple stem cell units is coordinated in response to local, heterogeneous tissue damage represents a fundamental question. By investigating how dispersed qNPs are locally recruited to injury, we have identified a mechanism that creates a defined zone of stem cell activation in the adult fly brain. The process is dependent on DNGCs, which depending on their size and possibly composition may regulate the extent by which a localized stem cell factor such as Wg/Wnt can travel to rare qNPs in the vicinity (Figure 6A). Whereas the neuronal cells provide Wg/Wnt, the glial component supplies the carrier protein Swim, thereby promoting the dispersion of the signal. To our knowledge, this cooperative interaction of two different cell types to gain long range function of Wg/Wnt is rather unique.

At the cellular level, we propose a model whereby injury-sensitive HIF1-α directs Swim synthesis in glial cells. Swim transporters diffuse and facilitate the spread of localized neural-derived Wg ligands, probably by binding to and shielding the

Please cite this article in press as: Simões et al., Damage-responsive neuro-glial clusters coordinate the recruitment of dormant neural stem cells in *Drosophila*, Developmental Cell (2022), https://doi.org/10.1016/j.devcel.2022.05.015

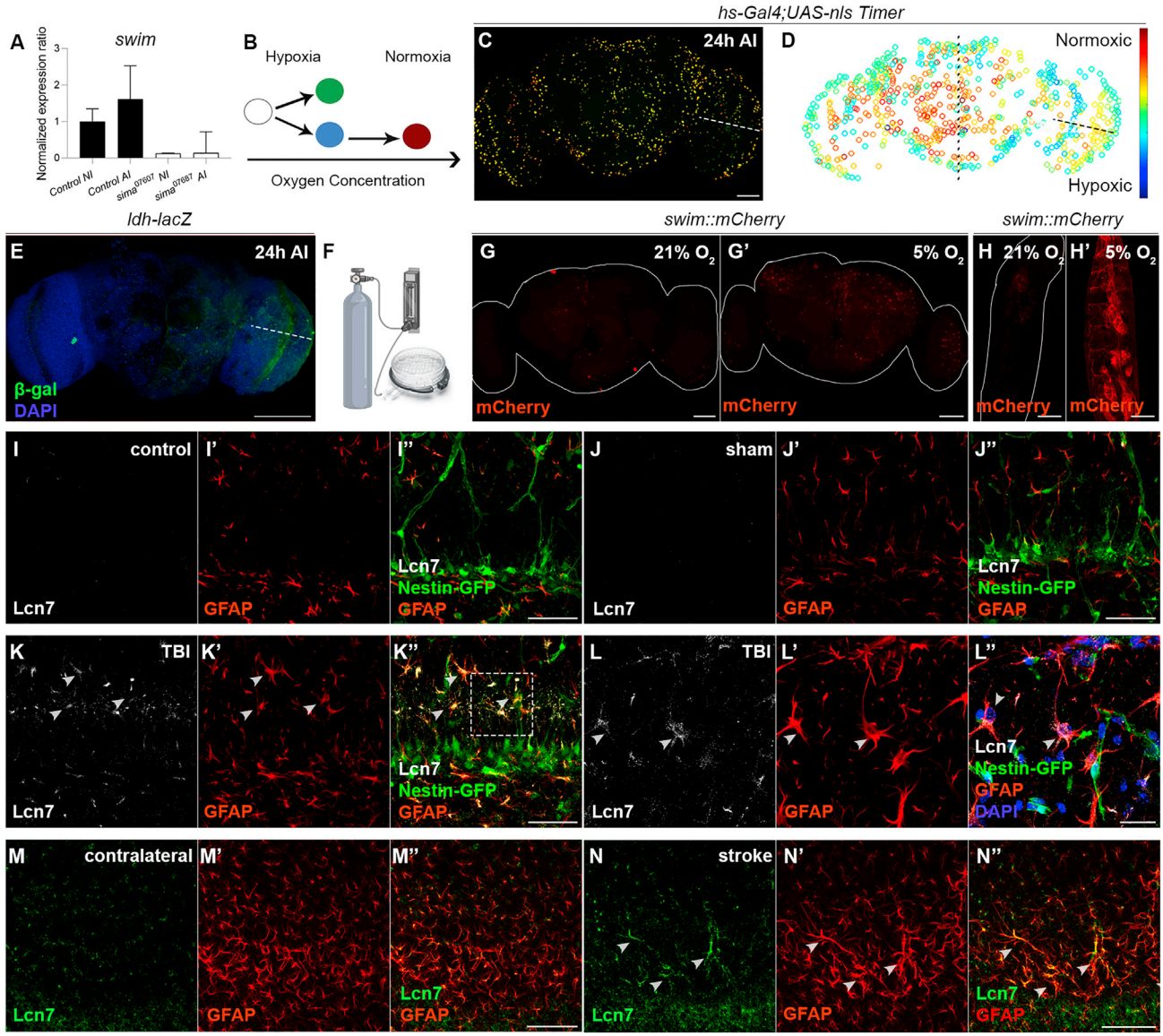

Figure 5. Brain injury induces glial expression of Swim/Lcn7 levels in flies and mice

(A) *Swim* qRT-PCR analysis in control (*Canton S*) and *sima*^{07607} null flies. Injured (AI), non-injured (NI). Error bars show SEM. n = 3.

(B) The oxygen sensor nlsTimer matures into a green fluorescent form or a blue fluorescent intermediate that slowly transforms into red fluorescence (Lidsky et al., 2018).

(C) Adult brain with induced nlsTimer expression (*hs-GAL4; UASt-nlsTimer*), 24 h after injury (AI). Overlay of acquired green and red channels.

(D) Histogram of calculated red/green ratios. Dashed line (right OL) indicates injury site.

(E) Expression of the hypoxia sensor *ldh-lacz* 24 h AI.

(F) Hypoxic chamber.

(G and H) Swim::mCherry induction (red) in the adult brain (G) and in larvae (H) under normoxic (21% O_2) and hypoxic conditions (5% O_2).

(I–K) Confocal sections of the dentate gyrus of *nestin-gfp* mice in control conditions (anesthesia) (I), following sham operation (exposed cortex) (J), and brain injury (cortical impact) 72 h after treatment (K). Neurons are shown in green (*nestin*-gfp), astrocytes in red (GFAP+), and Lcn7 staining in white. (L) Inset showing colocalization of Lcn7 signal (white) with astrocytes (GFAP+, red) following TBI. Neurons are shown in green, nuclei are stained with DAPI (blue). n = 3 brains (TBI), n = 2 (control), and n = 2 (sham).

(M and N) Lcn7 upregulation (green) in GFAP+ cells in the hippocampus on the contralateral side (M) and in the infarcted hemisphere (N) 72 h AI (n = 3 brains). Arrowheads point to GFAP+ glial cells with induced Lcn7 levels following ischemic brain injury. Scale bars: 20 μM (L), 50 μM (C), (G), (I)–(K), (M), and (N), 100 μM (E), and 500 μM (H).

lipid-residues of Wg/Wnt in the aqueous extracellular space (Figure 6B). Mobile Wg-Swim complexes are consequently able to reach and activate qNPs in the injured brain domain. We show that Wg/Wnt signal transduction and downstream upregulation of *dmyc* is crucial for the proliferation of this novel cell type. Overall, we propose that the described mechanism provides a means

Please cite this article in press as: Simões et al., Damage-responsive neuro-glial clusters coordinate the recruitment of dormant neural stem cells in *Drosophila*, Developmental Cell (2022), https://doi.org/10.1016/j.devcel.2022.05.015

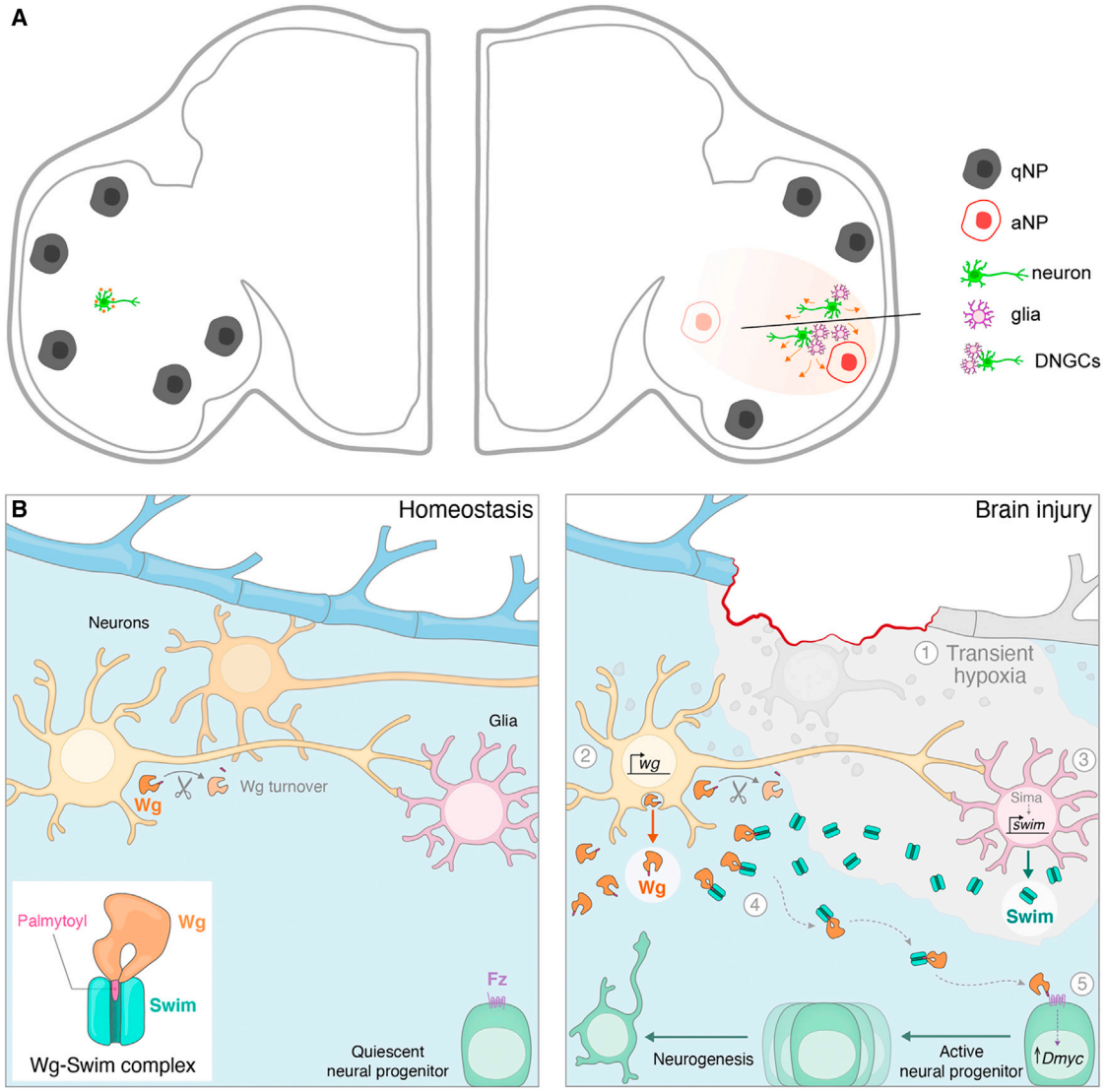

Figure 6. Model of injury-induced recruitment of qNPs

(A) Schematic view of intact (left) and injured adult *Drosophila* brain (right). Under homeostatic conditions, neural progenitors are mainly present in a quiescent state (qNP). Upon localized brain injury, damage-responsive neuro-glial clusters (DNGCs) promote the mobilization of neuron-derived Wg via glial-supplied Swim transporters. The extension and duration of the resulting stem cell activation zone (orange) depends on the availability of Swim, which in turn is regulated by the injury-sensing transcription factor Hif1-α.

(B) Inset on a neuro-glial cluster and nearby NP: glia in the injured brain area respond to transient hypoxia by upregulation of the secreted Wg-transporter Swim in a Sima/HIF1-α-dependent manner. Swim binding to hydrophobic Wg promotes its distribution in the injured brain area enabling activation of distant qNPs. High levels of Wg signaling in qNPs and downstream upregulation of *Drosophila* Myc (dMyc) promote proliferation. Inset depicts a putative Swim-Wg complex.

to match recruited stem cell activity to the spatial and temporal persistence of damage in the injured brain.

Activation of dormant neural progenitors by high levels of Wg/Wnt

Wg/Wnt signaling is probably one of the most universal pathways driving stem cell proliferation. Nevertheless, an understanding of Wg/Wnt signals for dormant stem cells has only recently emerged. Dormant muscle stem cells, for example, maintain quiescence by raising their threshold for Wnt transduction via cytoplasmic sequestration of β-catenin (Fuchs and Blau, 2020), and qNSC in the hippocampus do not rely on Wnt signaling under homeostasis but display a high capability to respond to Wnt in a graded manner when exposed (Austin et al., 2021). Similarly, our results demonstrate that qNPs start proliferating when high Wg/Wnt levels are provided in an autocrine fashion.

Overall, our results suggest that activation of qNPs in the adult fly brain is mainly prevented by the low availability of Wg/Wnt ligands under homeostatic conditions. Although Wnt signaling

Please cite this article in press as: Simões et al., Damage-responsive neuro-glial clusters coordinate the recruitment of dormant neural stem cells in *Drosophila*, Developmental Cell (2022), https://doi.org/10.1016/j.devcel.2022.05.015

normally occurs between adjacent cells (Nusse and Clevers, 2017), we provide evidence that Wg functions at a tissue scale in the injured fly brain.

Swim as a modulator of the local tissue environment

In this study, we describe the property of Swim to extend the signaling range of Wg/Wnt. Further research will be required to determine whether other stem cell-relevant factors can be transported by Swim.

In zebrafish, reduced levels of Swim/Lcn7 produce craniofacial defects due to compromised Wnt3 signaling (Neiswender et al., 2017), highlighting a different context of Wnt/Swim interaction. A Wg/Swim interaction has previously been proposed in developing epithelia in flies, although the effect was not observed in a more recent study (Mulligan et al., 2012; McGough et al., 2020).

We detected that Swim::mCherry is strongly expressed in the adult ovary germline of flies, in agreement with data from the recently published Fly Cell Atlas (Li et al., 2022) (Figure S6A). Remarkably, *swim* KO flies showed reduced fertility (Figure S6B), a phenotype which has also been reported for *lcn7/tinagl1* KO mice (Takahashi et al., 2016). Interestingly, Swim expression in the germarium strongly overlapped with Wg::GFP, in line with previous findings describing a requirement of extensive Wg travel from the niche to distant follicular stem cells (Wang and Page-McCaw, 2014) (Figure S6C).

HIF1-α-dependent Swim/Lcn7 modulation in the hypoxic brain

Finally, we elucidated how the Swim/Wg stem cell-activating signal is connected to damage sensing in the injured brain. Both in flies and mice, *swim/lcn7* induction occurs in glial cells in response to brain injury. Remarkably, stroke-induced *lcn7* induction is not observed in mouse brains, in which *Hif1-*α has been deleted from mature neurons and glial cells (Helton et al., 2005). This suggests that HIF1-α-dependent *swim* regulation is conserved in mammals.

According to our model, the damage responsiveness of stem cells is strongly gated by the availability of stable HIF1-α during acute hypoxia. Such a limited activation pulse would effectively restrict the mitotic effect of Swim/Wg complexes to the acute phase of repair, acting as a safeguard mechanism against overgrowth. Moreover, the hypoxia-dependent secretion of Swim would allow to temporally and locally fine-tune the realm of the stem cell activation zone to injury.

Local oxygen concentrations modulate the activity of adult stem cells in different niches (Mohyeldin et al., 2010). In the fly larval OL, Dpn-expressing neural progenitors proliferate in a pronounced hypoxic environment (Misra et al., 2017; Baccino-Calace et al., 2020), which bears parallels to the situation following brain injury.

In the mammalian brain, injury-induced Wnt ligands may not efficiently reach qNSCs in distant neurogenic niches, resulting in poor stem cell activation. As such, Wnt pathway stimulating approaches hold promise as possible treatment for brain injury as they are known to support regeneration at several levels including qNSC activation, neurogenesis, and axon outgrowth (Lambert et al., 2016). Increasing the mobility or stability of Wg/Wnts by Swim-like transporters may therefore represent a successful strategy to engage endogenous progenitors into regeneration. Given the fact that Wg/Wnts can support tissue renewal and regeneration in numerous tissues, the here-uncovered properties of Swim to transform a restricted tissue area into a temporary stem cell-activating zone may have important applications in regenerative medicine.

Limitations of the study

Although our experiments have revealed an impaired distribution of Wg in the injured brain in the absence of Swim transporters, we cannot completely rule out the possibility that Swim may alter Wg function by other means than physical binding and direct transport. Ideally, the injury-induced formation of Wg-Swim complexes should be observable in the extracellular space. Although we detected colocalization of Swim and Wg signals, we were not able to image Wg-Swim complexes at high resolution due to elevated background of Wg and mCherry antibodies when performing extracellular stainings. Overcoming these current limitations with overexpression systems or optimized immunodetection should allow to capture the dynamics of Wg-Swim interactions in injured brain tissue in the future.

STAR★METHODS

Detailed methods are provided in the online version of this paper and include the following:

- KEY RESOURCES TABLE
- RESOURCE AVAILABILITY
  - Lead contact
  - Materials availability
  - Data and code availability
- EXPERIMENTAL MODEL AND SUBJECT DETAILS
  - Fly lines and maintenance
  - Mouse lines and maintenance
- METHOD DETAILS
  - Stab lesions *Drosophila*
  - Traumatic brain injury (TBI): Cortical impact
  - Stroke model (middle cerebral artery occlusion; MCAO)
  - Fly Immunohistochemistry and image analysis
  - Mouse immunohistochemistry and image analysis
  - Microarrays
  - FACS and RNAseq
  - qRT-PCR
  - Generation of *dpn::T2A::Gal4* line
  - Generation of *swim* KO and KI flies
  - Lineage tracing
  - EdU
  - Hypoxia experiments
  - Embryo preparation
- QUANTIFICATION AND STATISTICAL ANALYSIS
  - Quantification of proliferation
  - Quantification of egg laying
  - Quantification of survival assay after injury
  - Oxygen monitoring
  - Quantification of JNK volume
  - Statistics

SUPPLEMENTAL INFORMATION

Supplemental information can be found online at https://doi.org/10.1016/j.devcel.2022.05.015.

ACKNOWLEDGMENTS

We thank the Bloomington Stock Center, the VDRC and the DSHB for antibodies and fly stocks; Christian Bökel and Alisson Gontijo for advice with CRISPR; and Stefan Thor, Claude Desplan, Pablo Wappner, Andrea PageMcCaw, Jean-Paul Vincent, Yuh Nung Jan, Ginés Morata, Christian Lehner, Julia Cordero, Boris Egger, and Marc Freeman for sharing antibodies or fly stocks. We thank Eduardo Moreno for support with microarrays; Esha Madan and Boris Egger for advice with hypoxia assays; Raquel Tomás for help with target vector design and cloning; Carmo Soares for technical assistance; Maria Diaz de la Loza for graphical support; and Carlos Ribeiro for valuable discussions on the manuscript. This work has been supported by the Champalimaud Foundation, a Fundação para a Ciência e Tecnologia (FCT) research grant to C.R. (PTDC/BIA-MOL/31170/2017), an FCT PhD fellowship to A.R.S. (SFRH/BD/121028/2016), an FPI (MINECO) predoctoral fellowship to I.D., a MINECO PCIN-2016-128 (ERA-NET-NEURON III program) and SAF2-015-70866-R (with FEDER funds) to J.M.E, an FCT Scientific Employment Stimulus-2018 and PTDC/MED-IMU/0870/2020 to D.B. and grants from the European Research Council, Paul G. Allen Frontiers Group and Fundación la Caixa to H.V.-F., plus the infrastructure support from CONGENTO (project LISBOA-01-0145-FEDER-022170).

AUTHOR CONTRIBUTIONS

A.R.S., M.N., and C.S.A. performed experiments and analyzed data. I.F.-H. prepared samples for microarrays. M.B.S. analyzed RNA-seq data. H.V.-F. and J.M.E. coordinated mouse experiments. D.B. performed MCAO. I.D. performed TBI and immunohistochemistry. C.R. conceived experiments, analyzed data, and wrote the manuscript with contributions from the other authors.

DECLARATION OF INTERESTS

H.V.-F. is on the board of LiMM Therapeutics.

Received: October 11, 2021
Revised: March 31, 2022
Accepted: May 18, 2022
Published: June 17, 2022

REFERENCES

Alexandre, C., Baena-Lopez, A., and Vincent, J.-P. (2014). Patterning and growth control by membrane-tethered wingless. Nature *505*, 180–185. 10.1038/nature12879.

Apitz, H., and Salecker, I. (2014). A challenge of numbers and diversity: neurogenesis in the *Drosophila* optic lobe. J. Neurogenet. *28*, 233–249. 10.3109/01677063.2014.922558.

Araki, T., and Milbrandt, J. (1996). Ninjurin, a novel adhesion molecule, is induced by nerve injury and promotes axonal growth. Neuron *17*, 353–361. 10.1016/S0896-6273(00)80166-X.

Arvidsson, A., Collin, T., Kirik, D., Kokaia, Z., and Lindvall, O. (2002). Neuronal replacement from endogenous precursors in the adult brain after stroke. Nat. Med. *8*, 963–970. 10.1038/nm747.

Austin, S.H.L., Gabarró-Solanas, R., Rigo, P., Paun, O., Harris, L., Guillemot, F., and Urbán, N. (2021). Wnt/β-catenin signalling is dispensable for adult neural stem cell homeostasis and activation. Development *148*, dev199629. 10.1242/dev.199629.

Baccino-Calace, M., Prieto, D., Cantera, R., and Egger, B. (2020). Compartment and cell-type specific hypoxia responses in the developing *Drosophila* brain. Biol. Open *9*, bio053629. 10.1242/bio.053629.

Baena-Lopez, L.A., Alexandre, C., Mitchell, A., Pasakarnis, L., and Vincent, J.P. (2013). Accelerated homologous recombination and subsequent genome modification in *Drosophila*. Development *140*, 4818–4825. 10.1242/dev.100933.

Baena-Lopez, L.A., Franch-Marro, X., and Vincent, J.-P. (2009). Wingless promotes proliferative growth in a gradient-independent manner. Sci. Signal. *2*, ra60. 10.1126/scisignal.2000360.

Blanpain, C., and Fuchs, E. (2014). Stem cell plasticity. Plasticity of epithelial stem cells in tissue regeneration. Science *344*, 1242281. 10.1126/science.1242281.

Braun, S.M.G., and Jessberger, S. (2014). Adult neurogenesis: mechanisms and functional significance. Development *141*, 1983–1986. 10.1242/dev.104596.

Broderick, S., Wang, X., Simms, N., and Page-McCaw, A. (2012). *Drosophila* Ninjurin A induces nonapoptotic cell death. PLoS One *7*, e44567.

Calleja, M., Moreno, E., Pelaz, S., and Morata, G. (1996). Visualization of gene expression in living adult *Drosophila*. Science *274*, 252–255. 10.1126/science.274.5285.252.

Centanin, L., Ratcliffe, P.J., and Wappner, P. (2005). Reversion of lethality and growth defects in Fatiga oxygen-sensor mutant flies by loss of hypoxia-inducible factor-alpha/Sima. EMBO Rep *6*, 1070–1075. 10.1038/sj.embor.7400528.

Chaturvedi, D., Reichert, H., Gunage, R.D., and Vijayraghavan, K. (2017). Identification and functional characterization of muscle satellite cells in *Drosophila*. Elife *6*, e30107. 10.7554/eLife.30107.

Chiu, H., Hoopfer, E.D., Coughlan, M.L., Pavlou, H.J., Goodwin, S.F., and Anderson, D.J. (2021). A circuit logic for sexually shared and dimorphic aggressive behaviors in *Drosophila*. Cell *184*, 507–520.e16. 10.1016/j.cell.2020.11.048.

Crocker, K.L., Marischuk, K., Rimkus, S.A., Zhou, H., Yin, J.C.P., and Boekhoff-Falk, G. (2021). Neurogenesis in the adult *Drosophila* brain. Genetics *219*. iyab092. 10.1093/genetics/iyab092.

Davie, K., Janssens, J., Koldere, D., De Waegeneer, M., Pech, U., Kreft, Ł., Aibar, S., Makhzami, S., Christiaens, V., Bravo González-Blas, C., et al. (2018). A single-cell transcriptome atlas of the aging Drosophila brain. Cell *174*, 982–998.e20. 10.1016/j.cell.2018.05.057.

Diao, F., and White, B.H. (2012). A novel approach for directing transgene expression in *Drosophila*: T2A-Gal4 in-frame fusion. Genetics *190*, 1139–1144. 10.1534/genetics.111.136291.

Eivers, E., Fuentealba, L.C., Sander, V., Clemens, J.C., Hartnett, L., and De Robertis, E.M. (2009). Mad is required for wingless signaling in wing development and segment patterning in *Drosophila*. PLoS One *4*, e6543.

Erclik, T., Li, X., Courgeon, M., Bertet, C., Chen, Z., Baumert, R., Ng, J., Koo, C., Arain, U., Behnia, R., et al. (2017). Integration of temporal and spatial patterning generates neural diversity. Nature *541*, 365–370. 10.1038/nature20794.

Evans, C.J., Olson, J.M., Ngo, K.T., Kim, E., Lee, N.E., Kuoy, E., Patananan, A.N., Sitz, D., Tran, P., Do, M.T., et al. (2009). G-TRACE: rapid Gal4-based cell lineage analysis in *Drosophila*. Nat. Methods *6*, 603–605. 10.1038/nmeth.1356.

Fernández-Hernández, I., Marsh, E.B., and Bonaguidi, M.A. (2021). Mechanosensory neuron regeneration in adult *Drosophila*. Development *148*. dev187534. 10.1242/dev.187534.

Fernández-Hernández, I., Rhiner, C., and Moreno, E. (2013). Adult neurogenesis in *Drosophila*. Cell Rep *3*, 1857–1865.

Fuchs, E., and Blau, H.M. (2020). Tissue stem cells: architects of their niches. Cell Stem Cell *27*, 532–556. 10.1016/j.stem.2020.09.011.

Glasheen, B.M., Robbins, R.M., Piette, C., Beitel, G.J., and Page-McCaw, A. (2010). A matrix metalloproteinase mediates airway remodeling in *Drosophila*. Dev. Biol. *344*, 772–783. 10.1016/j.ydbio.2010.05.504.

Harris, R.E., Setiawan, L., Saul, J., and Hariharan, I.K. (2016). Localized epigenetic silencing of a damage-activated WNT enhancer limits regeneration in mature *Drosophila* imaginal discs. eLife *5*, e11588. 10.7554/eLife.11588.

Helton, R., Cui, J., Scheel, J.R., Ellison, J.A., Ames, C., Gibson, C., Blouw, B., Ouyang, L., Dragatsis, I., et al. (2005). Brain-specific knock-out of

hypoxia-inducible factor-1alpha reduces rather than increases hypoxic-ischemic damage. J. Neurosci. Off. J. Soc. Neurosci. *25*, 4099–4107. 10.1523/JNEUROSCI.4555-04.2005.

Hinzman, J.M., Wilson, J.A., Mazzeo, A.T., Bullock, M.R., and Hartings, J.A. (2016). Excitotoxicity and metabolic crisis are associated with spreading depolarizations in severe traumatic brain injury patients. J. Neurotrauma *33*, 1775–1783. 10.1089/neu.2015.4226.

Homem, C.C.F., Repic, M., and Knoblich, J.A. (2015). Proliferation control in neural stem and progenitor cells. Nat. Rev. Neurosci. *16*, 647–659. 10.1038/nrn4021.

Huang, J., Zhou, W., Dong, W., Watson, A.M., and Hong, Y. (2009). From the Cover: directed, efficient, and versatile modifications of the *Drosophila* genome by genomic engineering. Proc. Natl. Acad. Sci. USA *106*, 8284–8289. 10.1073/pnas.0900641106.

Inaki, M., Yoshikawa, S., Thomas, J.B., Aburatani, H., and Nose, A. (2007). Wnt4 is a local repulsive cue that determines synaptic target specificity. Curr. Biol. *17*, 1574–1579. 10.1016/j.cub.2007.08.013.

Jaakkola, P., Mole, D.R., Tian, Y.M., Wilson, M.I., Gielbert, J., Gaskell, S.J., von Kriegsheim, A., Hebestreit, H.F., Mukherji, M., Schofield, C.J., et al. (2001). Targeting of HIF-α to the von Hippel-Lindau ubiquitylation complex by O2-regulated prolyl hydroxylation. Science *292*, 468–472. 10.1126/science.1059796.

Jackman, K., Kunz, A., and Iadecola, C. (2011). Modeling focal cerebral ischemia *in vivo*. Methods Mol. Biol. *793*, 195–209.

Kato, K., Awasaki, T., and Ito, K. (2009). Neuronal programmed cell death induces glial cell division in the adult *Drosophila* brain. Development *136*, 51–59. 10.1242/dev.023366.

Konstantinides, N., Kapuralin, K., Fadil, C., Barboza, L., Satija, R., and Desplan, C. (2018). Phenotypic convergence: distinct transcription factors regulate common terminal features. Cell *174*, 622–635.e13. 10.1016/j.cell.2018.05.021.

Lambert, C., Cisternas, P., and Inestrosa, N.C. (2016). Role of Wnt signaling in central nervous system injury. Mol. Neurobiol. *53*, 2297–2311. 10.1007/s12035-015-9138-x.

Lavista-Llanos, S., Centanin, L., Irisarri, M., Russo, D.M., Gleadle, J.M., Bocca, S.N., Muzzopappa, M., Ratcliffe, P.J., and Wappner, P. (2002). Control of the hypoxic response in *Drosophila* melanogaster by the basic helix-loop-helix PAS protein similar. Mol. Cell. Biol. *22*, 6842–6853. 10.1128/MCB.22.19.6842-6853.2002.

Leyssen, M., Ayaz, D., Hébert, S.S., Reeve, S., De Strooper, B., and Hassan, B.A. (2005). Amyloid precursor protein promotes post-developmental neurite arborization in the *Drosophila* brain. EMBO J *24*, 2944–2955. 10.1038/sj.emboj.7600757.

Li, G., Forero, M.G., Wentzell, J.S., Durmus, I., Wolf, R., Anthoney, N.C., Parker, M., Jiang, R., Hasenauer, J., Strausfeld, N.J., et al. (2020). A Toll-receptor map underlies structural brain plasticity. eLife *9*, e52743. 10.7554/eLife.52743.

Li, H., Janssens, J., De Waegeneer, M., Kolluru, S.S., Davie, K., Gardeux, V., Saelens, W., David, F.P.A., Brbić, M., Spanier, K., et al. (2022). Fly Cell Atlas: a single-nucleus transcriptomic atlas of the adult fruit fly. Science *375*, eabk2432. 10.1126/science.abk2432.

Lidsky, P.V., Lukyanov, K.A., Misra, T., Handke, B., Mishin, A.S., and Lehner, C.F. (2018). A genetically encoded fluorescent probe for imaging of oxygenation gradients in living *Drosophila*. Development *145*. dev156257. 10.1242/dev.156257.

Lim, T.K., Shi, X.Q., Johnson, J.M., Rone, M.B., Antel, J.P., David, S., and Zhang, J. (2015). Peripheral nerve injury induces persistent vascular dysfunction and endoneurial hypoxia, contributing to the genesis of neuropathic pain. J. Neurosci. *35*, 3346–3359. 10.1523/JNEUROSCI.4040-14.2015.

Llorens-Bobadilla, E., Zhao, S., Baser, A., Saiz-Castro, G., Zwadlo, K., and Martin-Villalba, A. (2015). Single-cell transcriptomics reveals a population of dormant neural stem cells that become activated upon brain injury. Cell Stem Cell *17*, 329–340. 10.1016/j.stem.2015.07.002.

MacDonald, J.M., Beach, M.G., Porpiglia, E., Sheehan, A.E., Watts, R.J., and Freeman, M.R. (2006). The *Drosophila* cell corpse engulfment receptor Draper mediates glial clearance of severed axons. Neuron *50*, 869–881. 10.1016/j.neuron.2006.04.028.

Magnusson, J.P., Göritz, C., Tatarishvili, J., Dias, D.O., Smith, E.M., Lindvall, O., Kokaia, Z., and Frisén, J.A. (2014). A latent neurogenic program in astrocytes regulated by Notch signaling in the mouse. Science *346*, 237–241. 10.1126/science.346.6206.237.

Marinho, J., Casares, F., and Pereira, P.S. (2011). The *Drosophila* Nol12 homologue viriato is a dMyc target that regulates nucleolar architecture and is required for dMyc-stimulated cell growth. Development *138*, 349–357. 10.1242/dev.054411.

McGough, I.J., Vecchia, L., Bishop, B., Malinauskas, T., Beckett, K., Joshi, D., O'Reilly, N., Siebold, C., Jones, E.Y., and Vincent, J.P. (2020). Glypicans shield the Wnt lipid moiety to enable signalling at a distance. Nature *585*, 85–90. 10.1038/s41586-020-2498-z.

Misra, T., Baccino-Calace, M., Meyenhofer, F., Rodriguez-Crespo, D., Akarsu, H., Armenta-Calderón, R., Gorr, T.A., Frei, C., Cantera, R., Egger, B., et al. (2017). A genetically encoded biosensor for visualising hypoxia responses *in vivo*. Biol. Open *6*, 296–304. 10.1242/bio.018226.

Mohyeldin, A., Garzón-Muvdi, T., and Quiñones-Hinojosa, A. (2010). Oxygen in stem cell biology: a critical component of the stem cell niche. Cell Stem Cell *7*, 150–161. 10.1016/j.stem.2010.07.007.

Morata, G., and Lawrence, P.A. (1977). The development of wingless, a homeotic mutation of *Drosophila*. Dev. Biol. *56*, 227–240. 10.1016/0012-1606(77)90266-4.

Moreno, E., Fernandez-Marrero, Y., Meyer, P., and Rhiner, C. (2015). Brain regeneration in *Drosophila* involves comparison of neuronal fitness. Curr. Biol. *25*, 955–963.

Mulligan, K.A., Fuerer, C., Ching, W., Fish, M., Willert, K., and Nusse, R. (2012). Secreted Wingless-interacting molecule (Swim) promotes long-range signaling by maintaining Wingless solubility. Proc. Natl. Acad. Sci. USA *109*, 370–377. 10.1073/pnas.1119197109.

Nagoshi, E., Sugino, K., Kula, E., Okazaki, E., Tachibana, T., Nelson, S., and Rosbash, M. (2010). Dissecting differential gene expression within the circadian neuronal circuit of *Drosophila*. Nat. Neurosci. *13*, 60–68. 10.1038/nn.2451.

Neiswender, H., Navarre, S., Kozlowski, D.J., and LeMosy, E.K. (2017). Early craniofacial defects in zebrafish that have reduced function of a Wnt-interacting extracellular matrix protein. Tinagl1. Cleft Palate Craniofac. J. *54*, 381–390. 10.1597/15-283.

Nériec, N., and Desplan, C. (2016). From the eye to the brain: development of the *Drosophila* visual system. Curr. Top. Dev. Biol. *116*, 247–271. 10.1016/bs.ctdb.2015.11.032.

Neumann, C.J., and Cohen, S.M. (1996). Distinct mitogenic and cell fate specification functions of wingless in different regions of the wing. Development *122*, 1781–1789. 10.1242/dev.122.6.1781.

Ng, S.Y., and Lee, A.Y.W. (2019). Traumatic brain injuries: pathophysiology and potential therapeutic targets. Front. Cell. Neurosci. *13*, 528. 10.3389/fncel.2019.00528.

Nusse, R., and Clevers, H. (2017). Wnt/b-catenin signaling, disease and emerging therapeutic modalities. Cell *169*, 985–999. 10.1016/j.cell.2017.05.016.

Pérez-Garijo, A., Shlevkov, E., and Morata, G. (2009). The role of Dpp and Wg in compensatory proliferation and in the formation of hyperplastic overgrowths caused by apoptotic cells in the *Drosophila* wing disc. Development *136*, 1169–1177. 10.1242/dev.034017.

Perez-Perri, J.I., Dengler, V.L., Audetat, K.A., Pandey, A., Bonner, E.A., Urh, M., Mendez, J., Daniels, D.L., Wappner, P., Galbraith, M.D., et al. (2016). The TIP60 complex is a conserved coactivator of HIF1A. Cell Rep *16*, 37–47. 10.1016/j.celrep.2016.05.082.

Port, F., and Bullock, S.L. (2016). Augmenting CRISPR applications in *Drosophila* with tRNA-flanked sgRNAs. Nat. Methods *13*, 852–854.

Port, F., Chen, H.M., Lee, T., and Bullock, S.L. (2014). Optimized CRISPR/Cas tools for efficient germline and somatic genome engineering in Drosophila. Proc. Natl. Acad. Sci. USA *111*, E2967–E2976.

Ryoo, H.D., Gorenc, T., and Steller, H. (2004). Apoptotic cells can induce compensatory cell proliferation through the JNK and the wingless signaling pathways. Dev. Cell *7*, 491–501. 10.1016/j.devcel.2004.08.019.

Saikumar, J., Byrns, C.N., Hemphill, M., Meaney, D.F., and Bonini, N.M. (2020). Dynamic neural and glial responses of a head-specific model for traumatic brain injury in *Drosophila*. Proc. Natl. Acad. Sci. USA *117*, 17269–17277.

Schindelin, J., Arganda-Carreras, I., Frise, E., Kaynig, V., Longair, M., Pietzsch, T., Preibisch, S., Rueden, C., Saalfeld, S., Schmid, B., et al. (2012). Fiji: an open-source platform for biological-image analysis. Nat. Methods *9*, 676–682. 10.1038/nmeth.2019.

Schwartz, S., and Rhiner, C. (2018). Reservoirs for repair? Damage-responsive stem cells and adult tissue regeneration in *Drosophila*. Int. J. Dev. Biol. *62*, 465–471. 10.1387/IJDB.180056CR.

Semenza, G.L. (1998). Hypoxia-inducible factor 1: master regulator of O_2 homeostasis. Curr. Opin. Genet. Dev. *8*, 588–594. 10.1016/S0959-437X(98)80016-6.

Shannon, P., Markiel, A., Ozier, O., Baliga, N.S., Wang, J.T., Ramage, D., Amin, N., Schwikowski, B., and Ideker, T. (2003). Cytoscape: a software environment for integrated models of biomolecular interaction networks. Genome Res *13*, 2498–2504. 10.1101/gr.1239303.

Sousa-Nunes, R., Cheng, L.Y., and Gould, A.P. (2010). Regulating neural proliferation in the *Drosophila* CNS. Curr. Opin. Neurobiol. *20*, 50–57. 10.1016/j.conb.2009.12.005.

Suzuki, T., Takayama, R., and Sato, M. (2016). eyeless/Pax6 controls the production of glial cells in the visual center of *Drosophila* melanogaster. Dev. Biol. *409*, 343–353. 10.1016/j.ydbio.2015.12.004.

Takahashi, A., Rahim, A., Takeuchi, M., Fukui, E., Yoshizawa, M., Mukai, K., Suematsu, M., Hasuwa, H., Okabe, M., and Matsumoto, H. (2016). Impaired female fertility in tubulointerstitial antigen-like 1-deficient mice. J. Reprod. Dev. *62*, 43–49. 10.1262/jrd.2015-109.

Tetteh, P.W., Farin, H.F., and Clevers, H. (2015). Plasticity within stem cell hierarchies in mammalian epithelia. Trends Cell Biol *25*, 100–108. 10.1016/j.tcb.2014.09.003.

van Velthoven, C.T.J., and Rando, T.A. (2019). Stem cell quiescence: dynamism, restraint, and cellular idling. Cell Stem Cell *24*, 213–225. 10.1016/j.stem.2019.01.001.

Wang, X., and Page-McCaw, A. (2014). A matrix metalloproteinase mediates long-distance attenuation of stem cell proliferation. J. Cell Biol. *206*, 923–936. 10.1083/jcb.201403084.

Wells, J.M., and Watt, F.M. (2018). Diverse mechanisms for endogenous regeneration and repair in mammalian organs. Nature *557*, 322–328. 10.1038/s41586-018-0073-7.

Yaghmaeian Salmani, B., and Thor, S. (2020). Genetic mechanisms controlling anterior expansion of the central nervous system. Curr. Top. Dev. Biol. *137*, 333–361. 10.1016/bs.ctdb.2019.11.005.

Zhao, C., Deng, W., and Gage, F.H. (2008). Mechanisms and functional implications of adult neurogenesis. Cell *132*, 645–660. 10.1016/j.cell.2008.01.033.

Zwarts, L., Versteven, M., and Callaerts, P. (2012). Genetics and neurobiology of aggression in *Drosophila*. Fly *6*, 35–48. 10.4161/fly.19249.

STAR★METHODS

KEY RESOURCES TABLE

REAGENT or Resource	SOURCE	IDENTIFIER
Antibodies		
rat anti-Elav (1:20)	DSHB	RRID: AB_528218
mouse anti-Repo (1:20)	DSHB	RRID: AB_528448
rabbit anti-cleaved Dcp-1 (1:100)	Cell Signaling	RRID: AB_2721060
rabbit anti-phospho-H3 (1:50)	Cell Signaling	RRID: AB_331535
mouse anti-Wingless (1:20)	DSHB	RRID: AB_528512
guinea-pig anti-NijA (1:100)	gift from Andrea Page-McCaw Vanderbilt School of Medicine	N/A
mouse anti-Hts (1:100)	DSHB	RRID: AB_528070
mouse anti-MMP1 (1:10)	DSHB	RRID: AB_579779
mouse anti-MMP1 (1:10)	DSHB	RRID: AB_579780
rabbit anti-mCherry (1:200)	Abcam	RRID: AB_2571870
mouse anti-Draper (1:100)	DSHB	RRID: AB_2618105
rabbit anti-Deadpan (1:100)	gift from Juh Nung Jan Howard Hughes Medical Institute	N/A
guinea-pig anti-Deadpan (1:400)	gift from StefanThor University of Queensland	N/A
mouse anti-Svp (1:5)	DSHB	RRID: AB_2618079
mouse anti-Bsh (1:50)	gift from Claude Desplan New York University (Erclik et al., 2017)	N/A
rabbit anti-Tinagl1 polyclonal (1:200)	BioNova Scientifica	MBS2554055
mouse anti-GFAP	Sigma Aldrich	RRID: AB_477010
Alexa fluor 488 rabbit (1:250)	Invitrogen	RRID: AB_2576217
Alexa fluor 488 mouse (1:250)	Invitrogen	RRID: AB_138404
Alexa fluor 555 rat (1:250)	Invitrogen	RRID: AB_141733
Alexa fluor 555 rabbit (1:250)	Invitrogen	RRID: AB_2535850
Alexa fluor 555 mouse (1:250)	Invitrogen	RRID: AB_141822
Alexa fluor 647 guinea-pig (1:100)	Invitrogen	RRID: AB_141882
Alexa fluor 647 rat (1:100)	Abcam	RRID: AB_2566823
Alexa fluor 647 mouse (1:100)	Invitrogen	RRID: AB_2535805
DAPI (1:1000)	Thermo Scientific	N/A
TUNEL kit Terminal Transferase	Roche	03333566001
Biotin-16-dUTP	Roche	11093070910
Click-It EdU labeling Kit	Invitrogen	C10340
Streptavidin 647 (1:250)	Invitrogen	RRID: AB_2336066
Phalloidin 647 (1:200)	Invitrogen	A22287
chicken anti-beta Galactosidase (1:100)	Abcam	RRID:AB_307210
Chemicals		
VECTASHIELD mounting medium	Vector Laboratories Inc.	H-1000
VECTASHIELD mounting medium with DAPI	Vector Laboratories Inc.	H-1200 94010
DakoCytomation Fluorescent Mounting Medium	DakoCytomation, Carpinteria, CA	CS70330-2
10X Phosphate bovine saline	Fisher Scientific	46-013-CM
1x Phosphate bovine saline	Fisher Scientific	21-040-CV
Tritonx-100	Sigma-Aldrich	X100
Paraformaldehyde	Thermo Scientific	#28906

(*Continued on next page*)

Please cite this article in press as: Simões et al., Damage-responsive neuro-glial clusters coordinate the recruitment of dormant neural stem cells in *Drosophila*, Developmental Cell (2022), https://doi.org/10.1016/j.devcel.2022.05.015

Continued

REAGENT or Resource	SOURCE	IDENTIFIER
Water (RNA free)	Fisher BioReagents	BP561-1
RNAse Cleaner	Nzytech	MB16001
Isopropanol	Fisher BioReagents	C3H80
TRIzol Reagent	Thermo Scientific	#15596026
Direct-zol RNA Microprep	Zymo Research	R2061
SuperScript III First-Strand Synthesis SuperMix for qRT-PCR	Invitrogen	#11752-050
GoTaq qPCR	Promega	A6001
Proteinase K	Nzytech	MB01901
DreamTaq Green PCR Master Mix	Thermo Scientific	K1082
Phusion High-Fidelity DNA Polymerase	Thermo Scientific	F530S
Zymoclean Gel DNA Recovery	Zymo Research	D4001
Bleach	Aro	LIO917
Heptane	Sigma-Aldrich	246654-1L
Methanol	VWR	20847.307-2.5L
Indigo Carmine	Sigma-Aldrich	131164
DNQX	Sigma-Aldrich	D0540-25MG
TTX	Sigma	T8024-1MG
APV (AP5)	Sigma	A8064-5MG
Insulin	Sigma	I0516-5ML
Fetal Bovine Serum	Corning	35-079-cv
Papain	Worthington Biochemical Corporation	LK003176
Buffer RLT Plus	Qiagen	#1053393
Deposited data		
Microarray	NCBI (GEO: GSE196884)	GSE196884
Experimental models: Organisms/strains		
wg-gal4,UASgfp/Cyo	gift from Manuel Calleja Centro de Biología Molecular Severo Ochoa	N/A
w;nos-Cas9attp2/TM6C	Bestgene	N/A
wg::gfp	gift from Jean-Paul Vincent Francis Crick Institute (Port et al., 2014)	N/A
tub-gal80^{ts};repo-Gal4/TM2	this study	N/A
tub-gal80^{ts}/Cyo;actin-Gal4/TM6b	Rhiner lab	N/A
actin-Gal4/TM6b	BDSC	3954
tubulin-Gal4	BDSC	5138
hs-Gal4	gift from Eduardo Moreno Champalimaud Centre	N/A
nijA^{D3}	gift from Andrea Page-McCaw Vanderbilt University (Broderick et al., 2012)	N/A
UASCD8::gfp/Cyo	gift from Eduardo Moreno Champalimaud Centre	N/A
UASgfp$_{nls}$	BDSC	4776
UAS RNAi swim	VDRC	10730
UAS RNAi swim/TM3	VDRC	6618
UAS swim/TM3	BDSC	38415
UAS RNAi dally-like	BDSC	50540
UAS RNAi arrow	VDRC	6708
UAS RNAi *dpn*	VDRC	28299
UAS wg-IR/Cyo;UAS-wg-IR/TM6B	gift from Julia Cordero Wolfson Wohl Cancer Research Centre	N/A
UAS myc RNAi	VDRC	71133

(*Continued on next page*)

Please cite this article in press as: Simões et al., Damage-responsive neuro-glial clusters coordinate the recruitment of dormant neural stem cells in *Drosophila*, Developmental Cell (2022), https://doi.org/10.1016/j.devcel.2022.05.015

Continued

REAGENT or Resource	SOURCE	IDENTIFIER
UAS wg-HA/Tm6b	BDSC	5918
UAS TCF^{DN}	BDSC	4785
UAS fz^{DN}	BDSC	44221
UAS daxin/TM3	gift from Eduardo Moreno, Champalimaud Centre	N/A
UAS lacZ	gift from Eduardo Moreno, Champalimaud Centre	N/A
wg{KO; NRT-Wg}	gift from Ginés Morata, Centro de Biología Molecular Severo Ochoa (Alexandre et al., 2014)	N/A
wg^{1}	BDSC	2978
w^{1118}	BDSC	6598
sima^{07607} (homozygous)	gift from Pablo Wappner Instituto Leloir	N/A
swim$^{3.3}$ (*swim* KO)	this study	N/A
swim KI {swim KO; swim::mCherry}	this study	N/A
dpnT2A-Gal4	this study	N/A
tub-Gal80^{ts}	this study	N/A
UASnls-timer	gift from Christian Lehner University of Zurich (Lidsky et al., 2018)	N/A
w; ubi-GFP-ODD, ubi-mRFP.nls	gift from B. Egger Université de Fribourg	N/A
Canton S and Oregon-R flies (wild-type)	gift from Eduardo Moreno Champalimaud Centre	N/A
G-trace (w;P{UASRedStinger}4,P{UASFLP.D} JD1,P {Ubip63E(FRT.STOP)Stinger}9F6/CyO)*	BDSC	28281
ldh-lacZ	gift from Pablo Wappner Instituto Leloir (Lavista-Llanos et al., 2002)	N/A
w;alrm-Gal4/Cyo;Dr/TM3,Sb	gift from Marc Freeman Vollum Institute	N/A
Mz0709-Gal4	Marc Freeman Vollum Institute	N/A
If/Cyo;Repo-Gal4/TM6B	gift from Eduardo Moreno Champalimaud Centre	N/A
TRE-GFP-16	gift from Eduardo Moreno Champalimaud Centre	N/A
Oligonucleotides		
PCR*CamKII*-specific primer sequence, forward: TTACACCATCCCAACATAGTGC	Marinho et al., 2011	N/A
PCR*CamKII*-specific primer sequence, reverse: CAAGGTCAAAAACAAGGTAGTGATAG	Marinho et al., 2011	N/A
PCR *myc*-specific primer sequence, forward: ATGGCCCTTTACCGCTCTG	FlyPrimer Bank	Primer Bank ID# PP4159
PCR *myc*-specific primer sequence, reverse: ACACTTTCCATGTCCTCGATCT	FlyPrimer Bank	Primer Bank ID# PP4159
PCR *swim*-specific primer sequence, forward: CTCGATTCACAGACTGGGCT	Primer blast	N/A
PCR *swim*-specific primer sequence, reverse: GGTGGGATTCTTTAGACGCG	Primer blast	N/A
PCR *nijA*-specific primer sequence, forward: CACAAGAAGACCCTGGCTCA	Primer blast	N/A
PCR *nijA*-specific primer sequence, reverse: AAGGATGTTGTGAGCTCGTC	Primer blast	N/A

(*Continued on next page*)

Please cite this article in press as: Simões et al., Damage-responsive neuro-glial clusters coordinate the recruitment of dormant neural stem cells in *Drosophila*, Developmental Cell (2022), https://doi.org/10.1016/j.devcel.2022.05.015

Continued

REAGENT or Resource	SOURCE	IDENTIFIER
PCR*lsp2*-specific primer sequence, forward: TATGTGCACCCGGAGATGTT	Primer blast	N/A
PCR *lsp2*-specific primer sequence, reverse: TAGAAGAGACGCACCAGACC	Primer blast	N/A
PCR *wg*-specific primer sequence, forward: *GATTATTCCGCAGTCTGGTC*	Eivers et al. 2009	N/A
PCR *wg*-specific primer sequence, reverse: *CTATTATGCTTGCGTCCCTG*	Eivers et al. 2009	N/A
CRISPR *swim* sgRNAs 5' -687ATG, [TTTCTAGATATATTAGACGG**TGG**], -687bp from ATG	this paper	N/A
CRISPR *swim* sgRNAs 3'-33STOP, [TTGTAGTAGCTGTAGACGTA**GGG**], -8bp from STOP codon	this paper	N/A
Software		
Fiji	Schindelin et al., 2012	https://imagej.nih.gov/ij/
Zen Digital Imaging for Light Microscopy	ZEISS	RRID:SCR_013672
GraphPad Prism 8	GraphPad Software	http://www.graphpad.com/
Imaris	OXFORD Instruments	RRID:SCR_007370
Cytoscape	Shannon et al., 2003	https://www.cytoscape.org

RESOURCE AVAILABILITY

Lead contact

Further information and requests for resources and reagents should be directed to and will be fulfilled by the lead contact, Christa Rhiner (christa.rhiner@research.fchampalimaud.org).

Materials availability

All *Drosophila* stocks generated in this study are available by contacting the lead contact directly.

Data and code availability

- Microarray data have been deposited at GEO: GSE196884 and are publicly available as of the date of publication.
- This paper does not report original code.
- Any additional information required to reanalyze the data reported in this paper is available from the lead contact upon request.

EXPERIMENTAL MODEL AND SUBJECT DETAILS

Fly lines and maintenance

Drosophila melanogaster were raised and maintained in an incubator set at 25°C, 60% humidity with a 12 h light/12 h dark cycle or at 18°C when combined with *tub-gal80^{ts}*. Details of genotypes used in this study and their sources are described in the key resources table. Female flies were used for brain injury experiments.

Drosophila melanogaster strains used in this study are listed in the key resources table. *Drosophila* were reared on cornmeal agar medium made with these ingredients (3.5L): 280g molasses (barley malt), 70 g Beet syrup, 280 g cornflour, 63 g granulated yeast, 35 g Soy flour, 27g Agar-Agar, 3700ml boiling water. Propionic Acid (28ml) and 15% Nipagin (42ml) are added after cool down to 60°C.

Flies were raised at 25°C except for all crosses including *tub-Gal80^{ts}*, which were raised at 18°C and only 3-day-old adult flies were transferred to 29°C.

Mouse lines and maintenance

C57BL/6J mice were maintained with access to food and water ad libitum in a colony room that was maintained at a constant temperature (19–22°C) and humidity (40–50%) on a 12:12 h light/dark cycle. Mice were bred and maintained at the Champalimaud and Achucarro facilities under specific pathogen free conditions. All animals were C57BL/6J mice, 2 months old and their weight was around 30 g when entering brain injury experiments. Male mice were used. Littermates of the same sex were randomly assigned to experimental groups. The experimental procedures involving cortical impact were performed in compliance with the European Community Council Directive of November 24, 1986 (86/609/EEC) and were approved by the University of the Basque Country

(UPV/EHU) Ethics Committees (Leioa, Spain) and the Diputación Foral de Bizkaia (protocol reference CEEA M20/2015/236). The experimental procedures involving stroke induction were approved by the national health authority (DGS) and the Portuguese Science Foundation (FCT).

METHOD DETAILS

Stab lesions *Drosophila*

A thin sterile filament (∅ 0,1mm or 0,2mm, Fine Science Tools), wiped with 70% EtOH was introduced through the right eye of at least 3-4-day-old adult CO_2- anesthetized flies to the level of the medulla in the optic lobe as previously described (Fernández-Hernández et al., 2013). The site and depth of the stab lesion was monitored either via eye pigment deposits in the OL (weak fluorescence in the red channel) or by dipping the filament into a fluorescent food dye (Indigo carmine, Sigma-Aldrich, #131164) mixed with water.

Traumatic brain injury (TBI): Cortical impact

2-month-old C57BL/6J mice were subjected to a unilateral cortical contusion by controlled cortical impact (CCI). Mice were anesthetized with isoflurane (2%) and placed in a stereotaxic frame. The skull was exposed by a midline incision, and a $4mm^2$ craniotomy was made lateral to the sagittal suture and centered between bregma and lambda. The skull cap was removed without damage to the exposed underlying dura. The contusion device consisted of a computer controlled, pneumatically driven impactor fitted with a rounded stainless-steel tip 3mm in diameter (Precision Systems and Instrumentation, Fairfax, VA). Brain injury was delivered using this device to compress the cortex to a depth of 0.5mm (mild) or 1.0mm (severe) at a velocity of 3.5m/sec and 400ms duration. SurgiSeal was placed over the dura after injury, the skull cap replaced, and the incision sutured. Mouse brains were analyzed 72h after injury.

Stroke model (middle cerebral artery occlusion; MCAO)

2-month-old C57BL/6J mice were subjected to transient focal cerebral ischemia using an intraluminal filament model of MCAO (Jackman et al., 2011). Briefly, mice were anesthetized with 1.5–2% isoflurane, and rectal temperature was maintained at 37 ± 0.5 °C throughout surgery. A silicone rubber-coated monofilament of 0.22 +/- 0.02 mm of diameter (Doccol Corporation, Sharon, MA, USA) was inserted into the right external carotid artery and advanced until it obstructed the MCA together with the ligation of the common carotid artery for 40 min. Obstruction of MCA was verified by measuring blood flow through laser doppler at the MCA territory (2mm posterior, 5 mm lateral to bregma). Only animals with $\geq$80 reduction of blood flow during MCAO and animals with $\geq$ 75% reperfusion after removing the filament were included. Following MCAO, mice were placed in temperature-controlled recovery cages for 2 hours to prevent post-surgery hypothermia. Mouse brains were analyzed 72h after injury.

Fly Immunohistochemistry and image analysis

Fly brains were dissected in chilled PBS, fixed in 4% PFA for 20 min at RT, washed with PBS-Triton-X 0.4% and incubated with primary (overnight at 4°C) and secondary antibodies (overnight at 4°C). Adult brains were mounted with a spacer to avoid compression of optic lobes. The antibodies used are described in the key resources table. For PH3 staining, samples were fixed overnight at 4°C in 2%PFA, washed and incubated for 48h/72h with primary Ab. For Deadpan staining, brains were fixed in 4% PFA for 30 min at RT, washed with PBS-Triton-X 1%, blocked for 1h with 5% FBS/1% PBS-T and incubated with primary Ab for 48h-72h at 4°C, washed and incubated with secondary Ab for 48h. To detect apoptotic cells, brains were dissected 48h and 72h after damage to perform TUNEL labeling (TUNEL kit, Roche). Samples were imaged on an 880 Zeiss confocal microscope.

Mouse immunohistochemistry and image analysis

For TBI samples, mice were deeply anesthetized and perfused with 30ml of PBS followed by 30 ml of 4% (w/v) paraformaldehyde in PBS, pH 7.4. The brains were postfixed, with the same fixative, for 3h at RT, then transferred to PBS and kept at 4°C. Serial 50 μm-thick sagittal sections were cut using a Leica VT 1200S vibrating blade microtome (Leica Microsystems GmbH, Wetzlar, Germany). Sections were incubated with blocking and permeabilization solution (PBS/0.25% Triton-100X and 3% BSA) for 3hr at RT, then incubated overnight with the primary antibodies at 4°C. After thorough washing with PBS, the sections were incubated with fluorochrome-conjugated secondary antibodies 4°C overnight. After washing with PBS, the sections were mounted on gelatin coated slides with DakoCytomation Fluorescent Mounting Medium. The antibodies used are described in the key resources table. Images were acquired using a Leica SP8 (Leica, Wetzlar, Germany) (TBI) or 880 Zeiss confocal microscope (stroke). The signal from each fluorochrome was collected sequentially, and controls with sections stained with single fluorochromes were performed to confirm the absence of signal leaking into different channels and antibody penetration. All images were imported into Adobe Photoshop 7.0 (Adobe Systems Incorporated, San Jose, CA) in tiff format. Brightness, contrast, and background were adjusted equally for the entire image using the "brightness and contrast" and "levels" controls from the "image/adjustment" set of options without any further modification. Al images shown are projections from z-stacks ranging from 10 (typically for individual cell images) to 20 microns of thickness.

Microarrays

7-day-old adult wild-type flies (Oregon-R) were injured on the right optic lobe with a stab lesion or left non-injured (controls) and kept at 25°C. 48h after damage, brains (with the lamina removed) were collected in chilled PBS, transferred to TRIzol and snap frozen.

Please cite this article in press as: Simões et al., Damage-responsive neuro-glial clusters coordinate the recruitment of dormant neural stem cells in *Drosophila*, Developmental Cell (2022), https://doi.org/10.1016/j.devcel.2022.05.015

Experimental and control samples (25 brains each) were prepared in quadruplicates. Samples were sent to the FlyChip *Drosophila* functional genomics unit (Cambridge) for extraction of total RNA, reverse transcription and labeling and hybridization to *Drosophila* whole transcriptome long-oligonucleotide array FL003 (GEO:GPL14121). Dye-swapping (2 arrays Cy5, 2 arrays Cy2) was performed to control for bias due to dye allocation. Genes showing at least fold change of -1.3 $\leq$ FC $\geq$ 1.3 and with p-value of $\leq$0.05 were selected for further bioinformatic analyses. Gene ontology analyses and enrichment was performed based on STRING and networks visualized with Cytoscape. Redundancy of the GO-terms was reduced with ReviGO.

FACS and RNAseq

Glial cells (*repo-Gal4; UASgfp*) and neurons (*elav-Gal4; UASgfp*) were harvested from 5 intact and injured (48hAI) adult fruit fly brains for three biological replicates. Adult brains were dissected and dissociated into single cell suspension as described by Nagoshi et al. (2010), adapted for OLs. For OL dissociation, OLs were incubated with 1μl/OL of activated Papain (Worthington Biochemical Corporation #LK003176) for 25 min at 25°C. Sample was subsequently dissociated using flame-rounded filter tips and passed through a sterile cell strainer (Fisherbrand® #22363548). 400 GFP-positive cells were sorted into PCR tubes (Axigen® #321-05-051) containing 2.5μl Buffer RLT Plus (Qiagen #1053393) by a calibrated BD FACS Aria Fusion (BD Biosciences, US) using a stringent single cell precision mask with a nozzle of 100μm. Tubes were placed on ice and immediately frozen at -80°C. Total RNA was extracted and processed with the SMART-SEQ2 protocol. RNA integrity was confirmed on an Agilent 2100 Bioanalyzer. Only RNA samples with A260/A280 > 2.0, an RNA integrity number (RIN) >7.0, and undetectable gDNA levels, were used for RNA-seq.

Libraries were generated with Nextera and sequenced using NextSeq500 Illumina systems. Clean reads were mapped to the *Drosophila melanogaster* reference genome (release 6 plus ISO1 MT) using STAR 2.7.0a. All subsequent analyses were done in RStudio (v1.4.1106; "Tiger Daylily" for Windows), based on Ensembl gene IDs. The conversion between gene id/names were finished with FlyBase ID converter (https://flybase.org/convert/id). Differentially expressed (DE) genes analysis was accomplished with R package DESeq2 (v1.31.16).

qRT-PCR

Total RNA was isolated from 30 adult fly brains using Direct-zol RNA Microprep (Zymo Research #R2061). After DNAse I treatment, cDNA was synthesized using the SuperScript III First-Strand Synthesis SuperMix. Each cDNA sample was amplified using GoTaq qPCR Master Mix on the CFX96 Real-Time System. Each experiment was performed at least three times. The relative quantification of each mRNA was performed using the comparative Ct method. The primers used in the qPCR analyses are described in the key resources table.

Generation of *dpn::T2A::Gal4* line

We used a CRISPR/Cas9-mediated homologous repair strategy to insert *T2A::Gal4* at the amino terminus of *dpn*. To this end, we cloned approx. 500 bp *dpn* homology arms (*dpn* C-terminus without stop and dpn 3′UTR respectively) into a pRK2-derived plasmid (Huang et al., 2009) (containing T2A::Gal4 sequences kindly provided by C. Boekel). A single *dpn* guide RNA and the plasmid containing *w+* as selection marker were injected into *w;nos-Cas9attp2/TM6C* flies. Transformants were balanced and the selection marker floxed-out by crossing founders to Cre line and further backcrossed.

Generation of *swim* KO and KI flies

We generated *swim* KO flies by CRISPR/Cas9-mediated gene editing. To this end, 1.5 kb 5′ and 3′ homology arms for *swim* were amplified from nos-Cas9 cDNA and sequenced, followed by directional cloning into pTV3 (gift of C. Alexander) containing attP- landing sites, mCherry transgenesis marker and flanking Cas9 recognition sequences for plasmid linearization upon injection.

The two guide RNAs (see key resources table) were cloned into the dual gRNA vector pCFD5 (Addgene #73914) by means of a ligation independent cloning (Port and Bullock, 2016). pTV3 and pCFD5 were then injected into nos-*Cas9* flies. Transformants were balanced and further crossed to Cre lines to flox-out the selection marker. The removed *swim* locus (total 2122bp) included the entire swim CDS plus a small stretch of upstream sequences (these were later reintroduced with the KI sequences). Primer sequences are available upon request.

To create *swim-mCherry* KIs flies at the *swim* KO locus, we amplified *swim* CDS (1435bp) plus 687bp upstream of the Swim ATG and inserted mCherry in frame before the *swim* stop codon. The *final swim::mCherry* was generated by means of Gibson Assembly and cloned into RIV-*white* vector (Baena-Lopez et al., 2013) between NotI and KpnI sites. Constructs were injected into homozygous *swim* KO flies.

Lineage tracing

For lineage tracing, *dpnT2A-Gal4; tub-Gal80^{ts}* flies were crossed to the G-trace stock and progeny was raised at 18°C. 3-day-old adult flies were shifted to 29°C for 24h, injured and placed back to 29°C and brains were dissected 24h after injury and 1 week AI.

EdU

For EdU labelling, 2-3-day-old adult flies were fed with 50μM of EdU in 10% Sucrose for 1 day, injured and placed again on EdU food until 72h AI. EdU solution was replaced every 24h. EdU signal was revealed using the Click-iT® EdU labelling kit (InVitrogen #C10640).

Please cite this article in press as: Simões et al., Damage-responsive neuro-glial clusters coordinate the recruitment of dormant neural stem cells in *Drosophila*, Developmental Cell (2022), https://doi.org/10.1016/j.devcel.2022.05.015

Hypoxia experiments

To create hypoxia, we purged the hypoxia chamber (Stem Cell Technologies) with a premixed pressurized gas of 5% oxygen in nitrogen according to the manufacturer's instructions. *Swim::mCherry* larvae (60h after larval hatching (ALH)) or adult flies were placed for 6h or 24h under hypoxia, respectively and the sealed chamber was transferred to 25°C. Larvae were immediately mounted in glycerol for microscopy without fixation; adult brains were fixed in 4% PFA/PBS and washed in PBS before mounting and imaging with confocal microscopy.

Embryo preparation

Eggs of *swim::mcherry* flies were dechorionated with 50% bleach in water for 3-4 min and rinsed with water and transferred to a glass scintillation vial containing 50% n-Heptane and 50% PFA 6% and incubated 20 min on a shaker. The lower phase was removed, an equal volume of methanol was added, and the tube immediately agitated for 15 s. The methanol phase was transferred to an Eppendorf using a glass Pasteur pipette and rinsed 3 times with methanol and 3 times with PBT before mounting. Embryos were staged and analyzed at stage 13-16.

QUANTIFICATION AND STATISTICAL ANALYSIS

Quantification of proliferation

For mitotic counts, RNAi was activated 4-5 days before injury by shifting flies to 29°C and brains were dissected 72h after stab lesion. DAPI-positive, PH3 dots were quantified in the adult optic lobes in equal settings across all samples. All PH3 positive cells were counted irrespective of signal intensity.

Quantification of egg laying

Sixteen virgin females and five 3-5 days-old males were transferred to apple juice plates, where they were allowed to lay eggs for 24h. Flies were removed, and egg laying was calculated by dividing the number of eggs by the number of living females at the end of the assay.

Quantification of survival assay after injury

30 w^{1118} and $swim^{3.3}$ KO female flies were collected right after eclosion. Flies were injured 24h after eclosion and maintained at 25°C on standard fly food, which was changed every 2 days. The number of living/death flies was counted every two-three days for 2 weeks.

Oxygen monitoring

Flies of genotype *hs-Gal4; UASnlstimer* were heat-shocked for 1h at 37°C and injured 24h afterwards. Brains were dissected 24h AI. For ratiometric analyses green and red channels were acquired below saturation and processed as previously described (Lidsky et al., 2018).

Quantification of JNK volume

The volume occupied by GFP+ stressed cells marked by *TRE::GFP* was quantified by using the manual setting of the Surfaces segmentation tool in Imaris to trace the outline of the injury zone and a surface was created. The same approach was used to assess the volume of the entire OL to subsequently determine the % of OL Volume filled by stressed cells.

Statistics

Results are shown as mean ± standard deviation (S.D) or standard error of the mean (S.E.M.). Statistical analyses were performed with GraphPad Prism software. Student's t-test was performed on homoscedastic populations. Results were considered significant at * $p < 0.05$; ** $p < 0.01$, *** $p < 0.001$, **** $p < 0.0001$.